

# Northumbria Research Link

Citation: Ting, Timothy Zhi Hong, Rahman, Muhammad and Lau, Hieng Ho (2020) Sustainable lightweight self-compacting concrete using oil palm shell and fly ash. *Construction and Building Materials*, 264. p. 120590. ISSN 0950-0618

Published by: Elsevier

URL: <https://doi.org/10.1016/j.conbuildmat.2020.120590>  
<<https://doi.org/10.1016/j.conbuildmat.2020.120590>>

This version was downloaded from Northumbria Research Link:  
<http://nrl.northumbria.ac.uk/id/eprint/45448/>

Northumbria University has developed Northumbria Research Link (NRL) to enable users to access the University's research output. Copyright © and moral rights for items on NRL are retained by the individual author(s) and/or other copyright owners. Single copies of full items can be reproduced, displayed or performed, and given to third parties in any format or medium for personal research or study, educational, or not-for-profit purposes without prior permission or charge, provided the authors, title and full bibliographic details are given, as well as a hyperlink and/or URL to the original metadata page. The content must not be changed in any way. Full items must not be sold commercially in any format or medium without formal permission of the copyright holder. The full policy is available online: <http://nrl.northumbria.ac.uk/policies.html>

This document may differ from the final, published version of the research and has been made available online in accordance with publisher policies. To read and/or cite from the published version of the research, please visit the publisher's website (a subscription may be required.)



**Northumbria  
University**  
NEWCASTLE



**UniversityLibrary**

# Sustainable Lightweight Self-compacting Concrete Using Oil Palm Shell and Fly Ash

Timothy Zhi Hong Ting<sup>1\*</sup>, Muhammad Ekhlalur Rahman<sup>1</sup> and Hieng Ho Lau<sup>2</sup>

<sup>1</sup>Department of Civil & Construction Engineering, Faculty of Engineering and Science,  
Curtin University, 98009 Sarawak, Malaysia

<sup>2</sup>Faculty of Engineering, Computing and Science, Swinburne University of Technology,  
93350 Sarawak, Malaysia

\*Correspondence: timothy.ting@postgrad.curtin.edu.my, Tel: +6085630100

Address: CDT 250, 98009 Miri, Sarawak, Malaysia

## **Abstract**

This research investigated fresh and hardened properties of lightweight self-compacting concrete (LWSCC) incorporated with oil palm shell (OPS) and fly ash (FA). Fresh concrete properties including passing ability, filling ability and segregation resistance were assessed. The properties fulfilled EFNARC guidelines. Incorporation of FA improved fresh properties, particularly filling ability, with the slump flow value increased from 665mm to 730mm. As for hardened properties, OPS-aggregate based LWSCC mixes achieved compressive strength of range 18-38MPa at 28-day age while the splitting tensile strength was in the range of 1.6 to 2.8MPa. SEM analyses showed good bonding in the interfacial transition zones (ITZ). Micropores of OPS were filled by cement hydration products and thus ITZ was enhanced. LWSCC incorporated with OPS, a renewable resource from agricultural waste, and with partial FA replacement, is potentially a sustainable alternative construction material.

Keywords: Oil palm shell, Fly ash, Fresh properties, Compressive strength, Splitting tensile strength, Interfacial transition zone, Water absorption

## 26 **1.0 Introduction**

27 Concrete is a most viable engineering material being used for construction [1]. For it to achieve  
28 designed strength and durability, fresh concrete has to be compacted in a proper way so as to  
29 make it homogeneous and dense. Compaction is normally done with the aid of vibrator during  
30 concreting and it raises concreting cost. In earnest quest for innovation in construction industry,  
31 Okamura and Ouchi [2] developed self-compacting concrete (SCC) in late 1980s and is  
32 gradually gaining popularity [3, 4]. SCC possesses properties to flow under gravity and more  
33 compactly fill the complex space of formwork as well as the area congested with reinforcement.  
34 Thus, it is not necessary to apply external concrete compaction method during casting of  
35 concrete. In accordance with the standards [5-7], SCC must possess characteristics of good  
36 durability, restrained flowing ability and filling ability with satisfactory resistance to  
37 segregation. In view of light weight structure, it is essential to utilize lightweight aggregates  
38 (LWA) to manufacture lightweight self-compacting concrete (LWSCC).

39 Normal weight aggregates (NWA), such as limestone, granite and sandstone are common  
40 materials used as coarse aggregates in concrete [8]. NWA is one of the (large) major  
41 constituents in concrete, be it normal concrete or SCC. Aggregates make up about 60% by  
42 volume in SCC and hence they are the main contributor to concrete weight [9]. About 20 billion  
43 tons of raw materials have been used for concrete production annually [10]. Aprianti [11]  
44 estimates the consumption of concrete will increase to 18 billion tons annually by 2050. As  
45 concrete production rate increases, NWA is gradually used up and thus causes its dwindling  
46 supply. The depleting supply of NWA can lead to significant hike in its cost as well as that of  
47 concrete. As such, it is of paramount importance that extensive research is to be carried out to  
48 develop more sustainable construction materials. Attempt has been made to utilise recycled  
49 aggregate from demolition waste [12-14]. Several recycle methods used include stock piling,  
50 crushing, presizing, sorting, screening and contaminant elimination. However, sizeable amount

51 of energy is entailed in processing recycled aggregates, leading to higher carbon dioxide  
52 emission. Moreover, it is difficult to produce concrete with desirable strength by using recycled  
53 aggregates as their mechanical properties are altered during recycling process.

54 Meanwhile, numerous contemporary research works [15-17] have dedicated to replacing NWA  
55 with lightweight aggregates (LWA). Generally, there are two categories of LWA, which are  
56 artificial type and natural type. Naturally sourced aggregates include pumice, diatomite,  
57 volcanic cinders, scoria and tuff [18, 19] while those in artificial category are classified into  
58 industrial by-products and modified natural arising materials [20, 21]. Industrial by-products  
59 such as sintered slate, sintered pulverized fuel ash, expanded or foamed blast furnace slag and  
60 colliery waste are commonly utilised as LWAs whilst naturally arising materials are shale,  
61 expanded clay, slate, vermiculite and perlite [22]. Undeniably, more benefits can be derived  
62 from utilising wastes to replace aggregates in concrete as it can reduce the environmental  
63 impacts with respect to waste reduction, pollution containment as well as less consumption of  
64 energy.

65 Mill processing of oil palm fruits will generate oil palm shell (OPS) as the main solid waste  
66 products [23, 24]. Palm nut yields two types of oil, which are palm oil and kernel oil and they  
67 are taken from outer and inner cores of the nut respectively. Palm kernel, which is produced  
68 from inner core of the nut after its oil has been extracted, is a potentially suitable coarse  
69 aggregate to be used in casting concrete. More common name for this palm kernel shell, which  
70 has an external hard endocarp, is oil palm shell [25]. Oil palm trees are abundantly cultivated  
71 in Malaysia. According to Tripathi et al. [26], Malaysia yields more than 52% of world's total  
72 palm oil. Land area of oil palm tree in Malaysia started with 54,000 hectares in 1960 and later  
73 increased to 5.90 million hectares in 2019 [27]. Huge quantities of OPS are being produced in  
74 oil palm mills with annual production of over 4 million tonnes [8, 20, 28]. This type of oil palm  
75 solid wastes is projected to increase as the demand for palm oil is increasing which leads to

76 increasing waste management issues. The present OPS disposal methods are incinerating and  
77 landfilling [29]. These two approaches not only are environmentally hazardous but also entail  
78 high capital outlay. As such, to mitigate environmental impacts with regard to the agricultural  
79 waste handling and disposing, much research has been conducted to utilise OPS [23, 24, 30,  
80 31] and agricultural wastes [32] as alternative materials. One very important aspect of the  
81 research is to utilise OPS as concrete constituents. According to Teo et al. [33], OPS can be  
82 incorporated into concrete as coarse aggregates.

83 For more than 3 decades, many researchers in South East Asia have been carrying out  
84 experiments in producing lightweight concrete by utilizing OPS [8]. Possessing porosity of 37%  
85 [23], OPS not only substantially reduces concrete density but also improves its thermal  
86 insulation property. Generally, by comparing to normal concrete, a density reduction of OPS  
87 concrete of about 20-25% is observed [31]. However, a negative effect of poor fresh concrete  
88 workability (low slump value) has been reported [23, 24, 34] in spite of using high water to  
89 cement ratio. The main reason for this is that OPS is irregular and flaky in shape. Nevertheless,  
90 the problem can be solved by incorporating some small quantity of superplasticizer which helps  
91 fresh concrete achieve desirable workability [35]. Subsequently, researchers in the related field  
92 attempt to develop OPS concrete by using superplasticizer as a constituent [36-38]. Yew et al.  
93 [39] conducted a study of the effects of OPS's age and size on concrete workability. By using  
94 age ranging from 3 to 15 years, older OPS was found to improve concrete workability.  
95 Nevertheless, decreasing maximum aggregate size from 12.5mm to 9.5mm decreased the  
96 workability. Explanation given by the authors was that full concrete compaction cannot be  
97 achieved due to irregular shapes of OPS caused by crushing process. To obtain optimum  
98 concrete workability, it is crucial that OPS with appropriate shape and right size gradation is  
99 selected. Meanwhile, Zawawi et al. [40] investigated the influence of fly ash blended with river  
100 sand as fine aggregate in OPS concrete. The authors concluded that the finer particle size of fly

101 ash as fine aggregate can result in degradation of workability of OPS concrete at high  
102 replacement level. As for OPS based self-compacting concrete, Prayuda et al. [41] studied the  
103 effect of granite replacement with OPS from 0% to 50% on V-funnel time. The results showed  
104 that the V-funnel time increased when OPS content increased, indicating degraded filling  
105 ability. Nevertheless, limited tests had been carried out by the authors to study the self-  
106 compacting ability of OPS based LWSCC. For hardened properties of OPS concrete, Okafor  
107 [24] reported that it was not possible to produce concrete with compressive strength higher  
108 than 30MPa if OPS was used as coarse aggregates. Meanwhile, other researchers also studied  
109 methods of treating OPS chemically [30, 42, 43] as well as using curing conditions [36, 44] to  
110 increase concrete compressive strength. Also, as shown by a few researchers, OPS concrete  
111 compressive strength above 30MPa can be attained through proper proportioning of  
112 constituents [45, 46]. OPS concrete with 28-day strength of 42-48MPa had been made by  
113 Shafigh et al. [47]. Shafigh et al. [36] were able to successfully achieve the compressive  
114 strength of 34-53MPa. Farahani et al. [48], in their more recent research, used binary and  
115 ternary blended cement to create OPS concrete with compressive strength 28-40MPa.  
116 Meanwhile, Alengaram et al. [49] found that OPS concrete specimens containing mineral  
117 admixtures possessed higher compressive strength than those without mineral admixtures. The  
118 authors argued that the mineral admixtures enhance the bond between the OPS and the matrix  
119 in the interfacial transition zone (ITZ) by filling the pores. The compressive strength of OPS-  
120 based concrete can be inferred to depend greatly on the bonding between (ITZ) of binder and  
121 aggregates phase. In all these studies, though, the higher strengths of the OPS concretes were  
122 made possible with the use of relatively large amount of cement or binder content. At this  
123 junction, it must be pointed out that, till now, no other researcher has attempted to use oil palm  
124 shell (OPS) to produce LWA in SCC.

125 With regard to the splitting tensile strength of OPS concrete, studies done by previous  
126 researchers [36, 48, 50] have shown that the value of splitting tensile strength possessed by  
127 OPS concrete is about 6-10% of its compressive strength. Alengaram et al. [51] argued that the  
128 weaker bonding between the aggregate matrix, when compared to normal aggregates concrete,  
129 has contributed to the low tensile strength of OPS concrete. By comparing the splitting tensile  
130 between normal concrete and OPS concrete, Shafigh et al. [36] found that the tensile splitting  
131 strength of OPS concrete is about 28% lower than that of normal aggregate concrete. Shafigh  
132 et al. [52] investigated the effect of high level fly ash replacement on splitting tensile strength  
133 of OPS concrete and found that, with 10% of fly ash replacement, the splitting tensile strength  
134 decreased by 19.7% though the compressive strength increased by 3.6%. The authors attributed  
135 poor tensile strength to poor material quality in interfacial transition zone (ITZ). With respect  
136 to water absorption, Teo et al. [33] reported that the water absorption of OPS based concrete  
137 was respectively 11.23% and 10.64% for concrete subjected to air-dry curing and full-water  
138 submerged curing. Shafigh et al. [47] reported that the water absorption of OPS concrete was  
139 in the range of 3-6%. Nevertheless, relatively high cement content was used to produce OPS  
140 concrete with low water absorption.

141 Comprehensive researches have been carried out in developing LWSCC by incorporating  
142 LWA from different sources [53]. In many cases, artificial LWA have been used. Also, many  
143 researchers have conducted extensive studies on incorporating LWA into SCC. Hwang and  
144 Hung [16] (utilized) incorporated reservoir fine sediment into SCC as coarse aggregates whilst  
145 Bogas et al. [54] and Hubertová and Hela [55] used expanded clay as concrete coarse  
146 aggregates. Using pumice as LWA in concrete had been studied under different temperature  
147 and with various mix proportions by a few researchers [56-61]. Also, Shi and Wu [62] and Lo  
148 et al. [63] have studied incorporation of expanded shale as coarse aggregates into SCC.  
149 However, limited research is being conducted with regard to incorporation of agricultural waste

150 into SCC. To date, no literature in respect of utilizing OPS as coarse aggregates for developing  
151 SCC has been published. All the related OPS concrete research is concerned on producing  
152 optimum lightweight concrete. In the meantime, Kanadasan and Razak [64] have been  
153 successful in utilizing oil palm clinker, which is also a type of oil palm waste, to make SCC.  
154 The authors have established an algorithm of SCC mix design by using particle packing  
155 concept. The mix design developed met the criteria of EFNARC [5] in respect to fresh concrete  
156 performance. Kanadasan and Abdul Razak [65] extended their study on SCC by utilizing palm  
157 oil clinker power as supplementary filler materials. It has been established that incorporation  
158 of oil palm clinker in SCC is sustainable in the aspects of energy efficiency and greenhouse  
159 gas emission.

160 Nevertheless, as mentioned by Mo et al. [37], it is necessary to use more cement in producing  
161 OPS concrete of anticipated compressive strength. In this regard, it will only make economic  
162 sense to use cheaper OPS in producing SCC in order to compensate for higher cost of bigger  
163 amount of cement required to achieve concrete self-compacting ability. Also, eradicating  
164 concrete vibration cost in SCC can further compensate for the extra cement material cost  
165 incurred. Moreover, fly ash, as supplementary cementitious material, if incorporated in  
166 concrete can not only improve the fresh state properties but also reduce cost. Produced by  
167 burning coal in furnaces of power plant, fly ash is considered as an industrial waste. Partial  
168 substitution of cement by fly ash is gaining popularity due to its ability to improve the fresh  
169 and hardened concrete properties. Bouzoubaa and Lachemi [66] reported that the use of  
170 superplasticizer tended to decrease when higher level of class F fly ash replacement was made.  
171 According to Khatib [67], workability improved with fly ash replacement up to 80%, by  
172 keeping constant both water-binder ratio and superplasticizer content in SCC. It has been stated  
173 by Ramanathan et al. [68] that partial substitution of cement with fly ash can lead to higher  
174 paste volume owing to its lower density, resulting in increased paste volume. Thus, friction at

175 the fine aggregate-paste interface is reduced. These can improve the cohesiveness and plasticity  
176 of concrete, resulting in improved workability. This trend has been similarly reported by Jalal  
177 et al. [69]. The hardened properties of concrete containing fly ash is highly depending on the  
178 level of fly ash replacement and class of fly ash. Generally, compressive strength of fly ash  
179 concrete at early age is generally lower than that of cement concrete. This has been  
180 demonstrated by numerous researchers [66-68] and is mainly due to slow-rate pozzolanic  
181 reaction of fly ash with calcium hydroxide in hydrated cement. Liu [70] also studied fly ash  
182 substitution up to 80% in SCC. The study was carried out up to 180 days. 20% fly ash  
183 replacement was found to be optimum in their study as the strength close to control concrete at  
184 the age of 90 days. Significant strength development was observed for high level fly ash  
185 replacement (above 60%) in the study. Atiş [71] also reported that 50% fly ash replacement in  
186 SCC can achieve comparable strength of control concrete.

187 Indeed, it is beneficial to utilize OPS and fly ash in concrete production, and as such, further  
188 research and development in the field will be continued with enthusiasm. To date, limited  
189 research has been carried out utilizing OPS as coarse aggregate in LWSCC. The utilization of  
190 OPS and fly ash in producing LWSCC could not only enhance its performance but also promote  
191 environmental sustainability in the aspect of waste utilization. The proposed LWSCC can  
192 effectively reuse biomass waste, reduce self-weight and avoid the need of external mechanical  
193 vibration of fresh concrete and hence is a more innovative construction material. Thus, the  
194 study in this paper is aimed at evaluating fresh and hardened properties of LWSCC  
195 incorporated with OPS as coarse aggregates. Control mix was determined based on particle  
196 packing method. Three levels of fly ash replacement (30%,40%,50%) was made to the control  
197 mixes. The resulting workability parameters including filling ability, passing ability and  
198 segregation resistance were evaluated. Compressive and splitting tensile strength of concrete  
199 were also determined.

200 **2.0 Experimental Programme**

201 **2.1 Materials**

202 The materials used for this experiment were supplied from the same source as Ting et al. [72].

203 **2.1.1 Ordinary Portland cement (OPC)**

204 Grade 45 Ordinary Portland Cement (OPC) which conforms to ASTM: C150/C150M-12, was  
205 used. Physical properties of OPC is presented in Table 1 while Table 2 shows the material  
206 chemical composition.

207 **Table 1: Physical properties of OPC**

<b>Physical properties</b>	<b>OPC</b>
Blaine fineness	3510 cm <sup>3</sup> /g
Specific gravity	3.14
Particle density	2950kg/m <sup>3</sup>

208

209 **2.1.2 Fly Ash**

210 The fly ash used in this study was acquired from a coal-fired power plant in Kuching, Sarawak,  
211 Malaysia and could be categorised as “Class F low calcium fly ash” in accordance to ASTM  
212 C618. The coal used in fly ash production was obtained from Merit Pila coal mine in Kapit,  
213 Sarawak, Malaysia. Table 2 shows chemical compositions of the cement and fly ash.

214 **Table 2: Chemical properties of cement and fly ash**

<b>Chemicals</b>	<b>Cement (%)</b>	<b>Fly Ash (%)</b>
Silicon dioxide (SiO <sub>2</sub> )	20.0	57.8
Aluminium oxide (Al <sub>2</sub> O <sub>3</sub> )	5.2	20.0
Ferric oxide (Fe <sub>2</sub> O <sub>3</sub> )	3.3	11.7
Calcium oxide (CaO)	63.2	3.28
Magnesium oxide (MgO)	0.8	1.95
Sulfur trioxide (SiO <sub>3</sub> )	2.4	0.08
K <sub>2</sub> O	-	3.88
TiO <sub>2</sub>	-	2.02
Na <sub>2</sub> O	-	0.30
Loss on ignition	2.5	0.32

215

216 **2.1.3 Coarse Aggregates**

217 Coarse aggregates used for concreting was Oil Palm Shell (OPS) which had been acquired  
218 from an oil palm processing mill in Miri, Sarawak, Malaysia. Physical properties of OPS are  
219 presented in Table 3. Specific gravity and water absorption of the OPS aggregate were  
220 determined in accordance with ASTM C127 [74] and ASTM C330 [75] respectively. The  
221 particle size distribution curve of OPS aggregates is shown in Figure 1. As for particle size  
222 distribution, OPS had 60% in size range of 5-10mm. After being washed and sieved, OPS had  
223 to be water submerged for a period of 24 hours. To obtain saturated surface dry (SSD) condition,  
224 OPS had to be air dried subsequently before being used for concreting purpose.

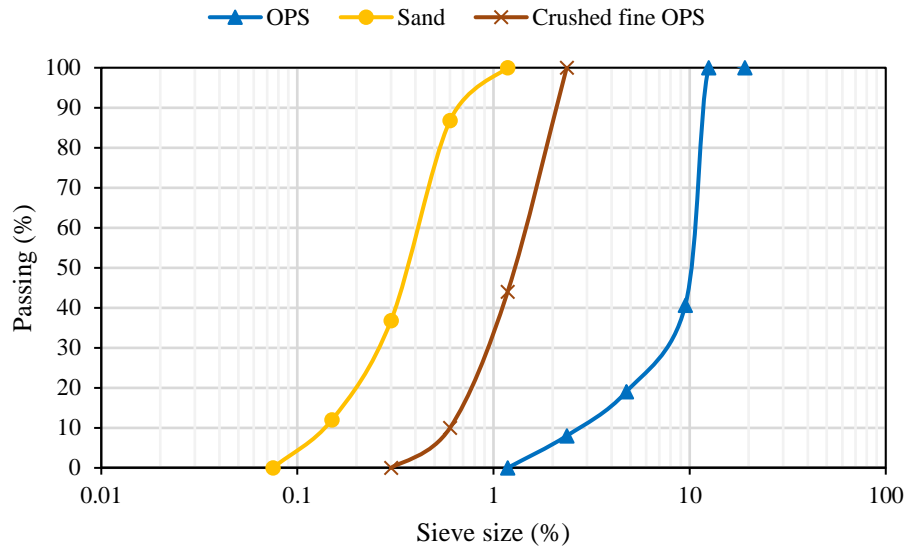
225 **2.1.4 Fine Aggregates**

226 Two types of fine aggregates used for this experiment were river sand and crushed OPS. OPS  
227 was crushed to the size range of 600µm to 5mm. Nominal size of river sand was 600µm.  
228 Physical properties of these two fine aggregates are shown in Table 3. Specific gravity and  
229 water absorption of the river sand were determined in accordance with ASTM C128 [76]. The  
230 particle size distribution curve of river sand is shown in Figure 1.

231 **Table 3: Physical properties of aggregates**

<b>Physical Property</b>	<b>River Sand</b>	<b>OPS</b>
Specific gravity	2.64	1.19
Fineness modulus	1.32	5.31
Water absorption (24h) (%)	1.1	18.11

232



233

234

**Figure 1: Particle size distribution of aggregates used**

235 **2.1.5 Superplasticizer**

236 In the experiment, Glenium Ace 389, a high range water reducing admixture obtained from  
 237 BASF Sdn. Bhd, was used. Categorized as Type F in ASTM C494 and BS En 934-2 European  
 238 Standard, it is can reduce water requirement for concreting by 12% or more.

239 **2.2 Mixing Method**

240 For concrete mixing, small type forced action cylindrical pan mixer with vertical rotation axis  
 241 had been used. Only about 0.07m<sup>3</sup> LWSCC was batched each time. First, both coarse and fine  
 242 aggregates were poured into the pan and the mixer was kept running for 1 minute. Then,  
 243 cement and fly ash were added and rotation of pan continued for another 2 minutes, until all  
 244 the materials were well mixed. Next, about 50% of the required amount of water was poured  
 245 into the pan slowly and the mixing continued for another 1 minute. Lastly, SP as well as the  
 246 other half amount of water were gradually poured in and the mixer was left running for a further  
 247 1 minute.

## 248 **2.3 Tests on Fresh Properties**

249 Concrete fresh properties including filling ability, passing ability and segregation were  
250 evaluated against European Federation of National Associations Representing for Concrete  
251 (EFNARC) [5] standard procedures. The proposed tests to evaluate the filling ability in this  
252 research were slump flow and V-funnel tests. The passing ability was assessed by J-ring test  
253 while segregation resistance was assessed through Sieve Segregation Test and Visual Stability  
254 Index (VSI). The detailed methodology to carry out all these fresh properties test was depicted  
255 in the following section.

### 256 **2.3.1 Slump Flow**

257 Slump flow test was proposed to assess the filling ability. Abram's slump cone with base  
258 diameter of 200mm and 300mm in height was used for slump flow test. Standard procedure  
259 for carrying slump flow test was to fill fresh concrete into a slump cone and the cone was then  
260 lifted up, permitting concrete to flow freely. The maximum uninterrupted flow diameters in  
261 two orthogonal directions were then measured after the flow had stopped.  $T_{500}$  was recorded  
262 as time taken for LWSCC to achieve 500mm diameter circular spread. The slump flow  
263 diameter was then calculated by using Eq. (1).

$$S = (d_{max} + d_{perp})/2 \quad (1)$$

264 where S is the slump value (mm),  $d_{max}$  is the maximum spread value (mm) and  $d_{perp}$  is the  
265 spread value perpendicular to the maximum spread.

### 266 **2.3.2 V-funnel Test**

267 V-funnel tests were also carried out to evaluate both the viscosity and filling ability of concrete.  
268 The shape of V-funnel restricts the flow of concrete and about 12 litres of concrete are required  
269 for the test to be carried out. The V-funnel was set on steel stand with bracing. Freshly prepared  
270 concrete was transferred to the V-funnel with trap door closed at bottom side. The trap door

271 was kept closed for 10 seconds after filling and then opened. The test was repeated for 5  
272 minutes after filling of V-funnel. The respective values of time taken after fresh LWSCC had  
273 flowed through V-funnel trap door were noted and recorded as  $T_{10s}$  and  $T_{5min}$ .

### 274 **2.3.3 J-ring Test**

275 Passing ability was evaluated through J-ring test. The purpose of this test was to assess  
276 blockage of LWSCC due to presence of steel bars. In carrying out the test, slump cone was  
277 placed at the centre of J-ring and fresh concrete was placed into the cone. Then, the cone was  
278 lifted up to let concrete to flow through steel bars. Maximum spread,  $T_{500 (J-Ring)}$ , and  
279 difference in height between the centre ( $h_1$ ) and outside of the ring ( $h_2$ ) were noted. Block step  
280 value ( $S_H$ ) can be calculated by using Eq. (2).

$$S_H = average(h_1 - h_2) \quad (2)$$

### 281 **2.3.4 Sieve Segregation Test**

282 Assessment of segregation resistance of fresh concrete was done through sieve segregation test.  
283 The test began by allowing the mass of fresh concrete to stand still in a container for 15 minutes.  
284 The mass of pan was then measured as  $W_p$  on weighing balance. The actual mass of LWSCC  
285 used was recorded as  $W_c$ . It was then poured into sieve and permitted to flow through sieve  
286 with 4.75mm aperture within 2-minute duration. The weight of concrete which passed through  
287 the sieve was recorded as  $W_{ps}$ . This value was computed as the percentage of total weight of  
288 LWSCC used by using Eq. (3).

$$\Pi = (W_{ps} - W_p)/W_c \times 100 \quad (3)$$

### 289 **2.3.5 Visual Stability Index Test**

290 Visual stability index (VSI) test was carried out by visual inspection of LWSCC before and  
291 after slump flow tests had been done. The index values varied from 0 to 3 [6]. However,

292 accuracy of this method heavily rely on the knowledge and experience of the individual  
 293 interpreting and evaluating segregation the results. The VSI criteria is adopted from PCI  
 294 guideline [78] and shown in Table 4.

295 **Table 4: VSI criteria [78]**

VSI	Criteria
0	No sign of concrete segregation or bleeding.
1	No sign of concrete segregation but with inconsiderable bleeding noticed as a sheen on the surface.
2	A slight mortar halo ( $\leq 10$ mm) and/or aggregate heave in the middle of the concrete mass and some bleeding.
3	Clear evidence of segregation in the form of a large mortar halo ( $\geq 10$ mm) and/or a large aggregate pile in the centre of the concrete mass.

296  
 297 **2.4 Test on Hardened Properties**

298 **2.4.1 Strength Test**

299 Concrete cube specimens with size of 100x100x100mm were casted and prepared for  
 300 compressive strength test. Meanwhile, splitting tensile test was done on 100mm diameter by  
 301 200mm height cylinders. When preparing the specimens, fresh concrete was mixed and poured  
 302 into two respective types of mould immediately after it had been tested for slump flow. All the  
 303 LWSCC specimens were allowed to self-compact without the aid of vibrator. 24 hours later,  
 304 the concrete specimens were demoulded. The specimens were cured in water before being  
 305 tested. All the cubes and cylinders were tested by using 600kN capacity GOTECH universal  
 306 testing machine. The compressive strength test was conducted in accordance with the standard  
 307 procedure described in ASTM C39-18 and BS 1181-116 for cylinder and cube respectively.  
 308 The method prescribed by Norma [81] was used to carry out splitting tensile strength test.

309 **2.4.2 Density**

310 The relevant values of concrete density were determined when it was demoulded, air-dried and  
 311 finally oven-dried. The demoulded density of concrete samples was determined immediately

312 after the removal of concrete mould. The air-dry density was determined after the demoulded  
313 sample had been air dried. Oven-dry density of LWSCC was determined through the test  
314 prescribed in ASTM C567-14. The apparent mass of cylinder (G) was measured when it was  
315 completely submerged in water. The cylinder was allowed to air dry for 1 minute and the  
316 surface water was using absorbent cloth. The mass was then recorded as saturated surface-dry  
317 cylinder (F). Concrete samples were then placed in an oven and continually weighted until  
318 there was minimal change in the weight. The final weight recorded under room temperature  
319 was mass of oven-dry cylinder (D). The Oven-dry density can be calculated by using Eq. (4).

$$O_m = (D \times 997)/(F - G) \quad (4)$$

### 320 **2.4.3 Immersed Water Absorption**

321 Immersed water absorption test was conducted according to the procedure prescribed in ASTM  
322 C642-13. In the experiment, the prepared sample was weighted and then allowed to oven dry  
323 at 110°C for 24 hours. The sample was weighted again at room temperature after oven drying  
324 process. If the difference between two successive measured weights was more than 1g, oven  
325 drying process had to be repeated until the difference was less than 1g. This value was noted  
326 as  $M_1$ . The sample was then immersed into water for 48 hours. After the immersion, concrete  
327 surface was dried using cloth. The mass was measured as  $M_2$ . The water absorption was  
328 computed by using Eq. (5).

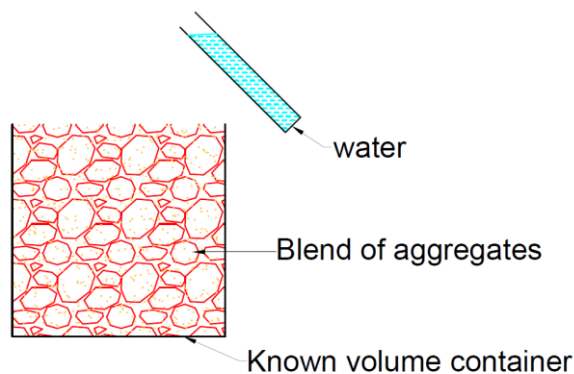
$$\text{Water absorption} = (M_2 - M_1)/M_1 \times 100 \quad (5)$$

### 329 **3.0 LWSCC Mix Design**

330 Presently, there is no standard method which can be used for the mix design of LWSCC.  
331 Nevertheless, for this study, a method proposed by Kanadasan and Razak [64], which was  
332 known as particle packing method, was adopted. This method assumed that the voids between  
333 aggregates particles are filled by paste. Figure 3 shows the overall mix design procedure.

334 **3.1 Particle Packing Method**

335 Particle packing (PP) is defined as volume of packed aggregate particles in a unit volume [84].  
336 The study is targeted at determining suitable LWSCC mix design method. The method  
337 recommends that PP test has to be carried out first. It is a prerequisite to pre-soak all the  
338 aggregates in water for 24 hours and air dry to saturated surface dry condition (SSD). Fixed  
339 amounts of fine and coarse aggregates are prepared and put into a container of known volume.  
340 The aggregates are mixed thoroughly so that they are well-blended. Known amount of water is  
341 added into the container until it is full, as illustrated in Figure 2. This volume of water  
342 represents total volume of voids in aggregates, which is equal to the required amount of paste  
343 to be used for proportioning LWSCC. The PP ratio is obtained by subtracting the void ratio  
344 from container volume.



345

346 **Figure 2: PP Test Illustration [64]**

347 **3.2 Mix Design Algorithm**

348 The procedures to determinate the LWSCC mix design is presented in this section.

349 Step 1: Determination of particle packing factor

350 The first step in proportioning LWSCC mix, which incorporates OPS as full coarse aggregates  
351 replacement, is to determine the particle packing factor between the blended OPS as coarse  
352 aggregates and river sand as fine aggregates, by using Eq. (6). The minimum paste volume

353 necessary for lubricating aggregates so as to produce the required characteristics of flowing  
354 and filling ability of LWSCC is represented by the voids [64]. Required amount of paste to fill  
355 OPS aggregate void is more with a lower value of PP ratio. On the other hand, a high PP ratio  
356 indicates that less paste is required as aggregates are tightly packed. The PP value is determined  
357 based on the procedure described in previous section.

$$PP = 1 - e \quad (6)$$

358 where PP is particle packing value and e is void ratio

359 Step 2: Calculation of aggregates content

360 The aggregate content of proposed LWSCC mix design can be determined from Eq. (7). The  
361 subscript of f/c agg in each term represents respective type of aggregate used and the ratio of  
362 each aggregate to total aggregates in a unit volume of LWSCC has been considered. The main  
363 concern of aggregates in this research is fine aggregate which is sand, and OPS as coarse  
364 aggregate. The optimum ratio of each aggregate to total aggregates was determined from the  
365 blended aggregates bulk density curve.

$$W_{f/c \text{ agg}} = PP \times AR_{f/c \text{ agg}} \times SG_{f/c \text{ agg}} \times 1000 \quad (7)$$

366 where  $W_{f/c \text{ agg}}$  is aggregate content ( $\text{kg/m}^3$ ),  $AR_{f/c \text{ agg}}$  is ratio of aggregate to total aggregates  
367 in volume and  $SG_{f/c \text{ agg}}$  is specific gravity of aggregates.

368 Step 3: Calculation of cement content

369 Cement content must be chosen properly to ensure the concrete fresh properties as a SCC,  
370 including filling ability, passing ability and segregation resistance, fulfil the specified  
371 requirements while not to compromise the compressive strength. Good adjustment of cement  
372 content will ensure sufficient amount of cement paste is available to lubricate aggregates so as  
373 to attain self-compacting ability. The volume of cement can be determined using Eq. (8).

$$V_{\text{cement}} = W_{\text{cement}}/SG_{\text{cement}} \quad (8)$$

374 where  $V_{\text{cement}}$  is volume of cement,  $W_{\text{cement}}$  is cement content ( $\text{kg}/\text{m}^3$ ) and  $SG_{\text{cement}}$  is  
375 specific gravity of cement.

376 Step 4: Calculation of paste volume

377 The voids that exist in particle packing of aggregates represent the amount of paste required to  
378 be filled to ensure good concrete self-compacting ability. This can be calculated by using Eq.  
379 (9).

$$V_{\text{paste}} = 1 - PP \quad (9)$$

380 where  $V_{\text{paste}}$  volume of paste

381 Step 5: Determination of water content

382 Water content can be calculated by water to binder (W/B) ratio using Eq. (10) and Eq. (11).  
383 The actual W/B needs to be validated and adjusted by trial mix.

$$V_{\text{water}}/V_{\text{cement}} = W/B \quad (10)$$

$$W_{\text{water}} = V_{\text{water}} \times SG_{\text{water}} \times 1000 \quad (11)$$

384 where W/B is water to binder ratio,  $V_{\text{water}}$  is volume of water content,  $W_{\text{water}}$  is water content  
385 ( $\text{kg}/\text{m}^3$ ) and  $SG_{\text{water}}$  is specific gravity of water.

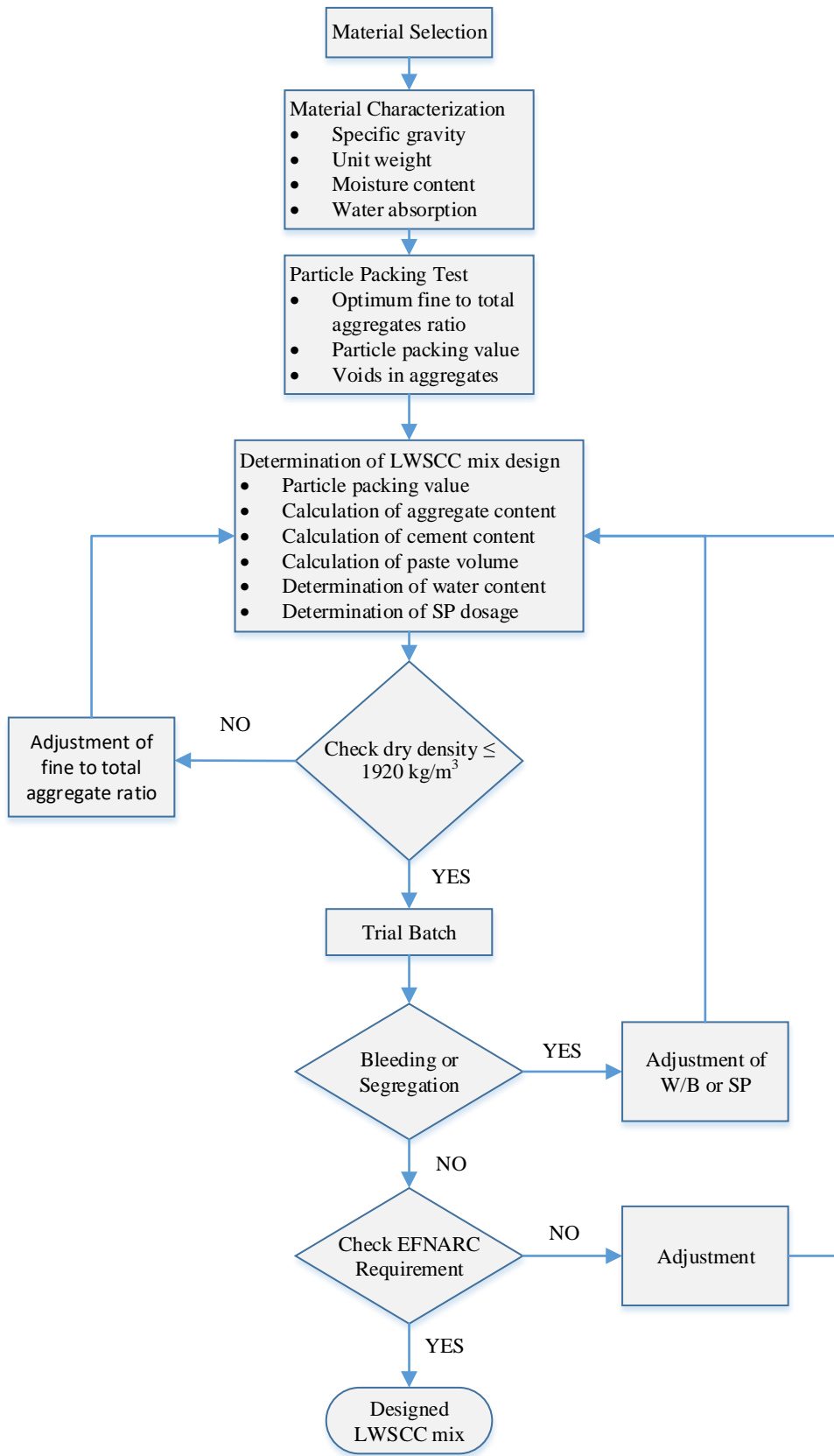
386 Step 6: Determination of superplasticizer dosage

387 SP is an essential constituent to allow SCC to achieve followability and passing ability.  
388 However, excessive dosage of SP can cause severe bleeding and segregation. Determination of  
389 optimum SP can help SCC achieve optimum performance. The SP content can be calculated  
390 by using Eq. (12). Adjustment of dosage has to be made if its fresh properties do not fulfil the  
391 criteria in the EFNARC [5].

$$W_{SP} = SP(\%) \times (W_{\text{cement}} + W_{\text{SCM}}) \quad (12)$$

392 where  $W_{SP}$  is superplasticizer content ( $\text{kg}/\text{m}^3$ ),  $SP(\%)$  is superplasticizer dosage and  $W_{SCM}$  is  
393 supplementary cementitious material content ( $\text{kg}/\text{m}^3$ ).

394 The mix proportion computed by using PP test is the baseline for designing LWSCC mix. It is  
395 also necessary to conduct fresh and hardened concrete tests to ascertain compliance to  
396 EFNARC [5]. The mix design is checked and fine tuned to the requirements in Annex C of  
397 BIM and ERMCO [85]. Flowchart for mix design is presented as Figure 3.



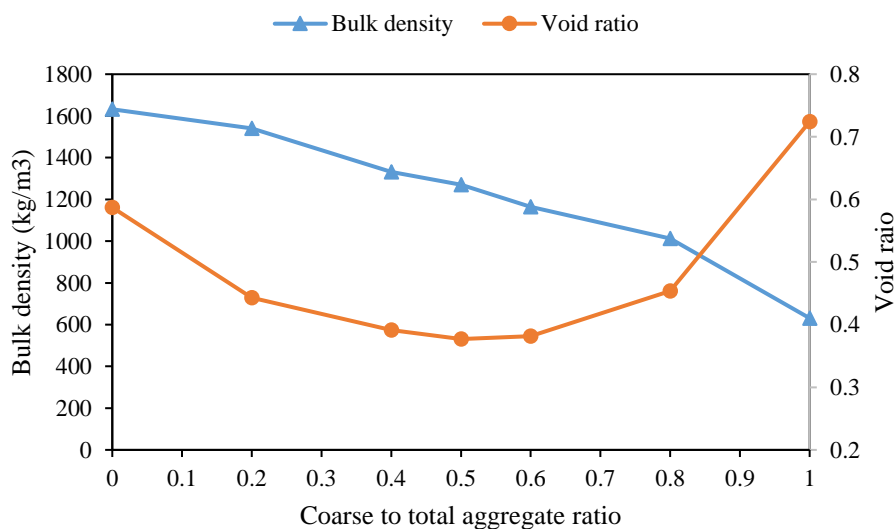
398

399

**Figure 3: Flowchart for achieving LWSCC mix design**

### 3.3 LWSCC Mix Proportion

Based on ASTM C29, the relationships between bulk density as well as void ratio and aggregates ratio were established in Figure 4. For bulk density versus coarse to total aggregate ratio, it is noted that the bulk density decreased with increasing coarse aggregate content. It is because coarse aggregate (OPS) has lower specific gravity compared to fine aggregates (river sand). Lowest void ratio can be observed when the coarse to fine aggregates ratio is 1:1. This indicates that ratio of 50% of coarse aggregate and 50% fine aggregate is the optimum aggregate content for OPS and river sand combination. When coarse to total aggregate ratio is increased from 0.5 to 0.6, even though the density decreases, the void ratio exhibits a rising trend. This rising trend indicates more paste is necessary for filling voids. Several researchers have used coarse to total aggregate ratios of 0.5 [64, 87] and 0.6 [62, 64, 88] in proportioning LWSCC. Cement content of  $520 \text{ kg/m}^3$  was chosen since OPS concrete requires more cement paste to facilitate self-compacting ability. Coarse to total aggregate ratio of 0.6 was chosen since it could reduce the density of proposed LWSCC and more economic mix is produced that can compensate the high cement content used.



415

416 **Figure 4: Influence of coarse to fine aggregate ratio on bulk density and void ratio**

417 Table 5 presents the finalized mix design to be studied. In this research, 30% to 50% of fly ash  
 418 replacements were made to the control mix. With the replacement of fly ash, water demand  
 419 was decreased, so as W/B was decreased from 0.33 to 0.31. The presence of fly ash was able  
 420 to improve the packing of LWSCC which in turn reduced the water demand although fly ash  
 421 exhibited characteristic of high affinity to water. The capability of fly ash to improve the  
 422 workability of LWSCC can be explained in terms of the spherical and smooth nature of fly ash  
 423 particles which induce the ball bearing effect. Partial replacement of cement by fly ash can  
 424 result in higher paste volume, which in turn reduces the friction at the fine aggregate-paste  
 425 interface. Consequently, the cohesiveness and plasticity of concrete improve [68]. Hence, the  
 426 improved concrete workability is achieved with lesser water demand. The comparison of these  
 427 four mix designs was made in the following section.

428 **Table 5: Summary of mix design**

Mix	M0	M30	M40	M50
<b>Cement (kg/m<sup>3</sup>)</b>	520	364	312	260
<b>Fly Ash (kg/m<sup>3</sup>)</b>	0	156	208	260
<b>Water (kg/m<sup>3</sup>)</b>	171.6	161.2	161.2	161.2
<b>Sand (kg/m<sup>3</sup>)</b>	715	715	715	715
<b>Coarse Aggregate (kg/m<sup>3</sup>)</b>	455	455	455	455
<b>SP (kg/m<sup>3</sup>)</b>	8.58	8.58	8.58	8.58
<b>Air content</b>	1%	1%	1%	1%
<b>Water to binder ratio</b>	0.33	0.31	0.31	0.31
<b>Coarse Aggregate to total aggregate ratio</b>	0.39	0.39	0.39	0.39

429

430 **4.0 LWSCC Mix Design**

431 **4.1 Fresh Properties**

432 Guidelines for carrying out SCC workability tests have been formulated in several publications  
 433 such as EFNARC [5] and ACI-237 [7]. In this study, all the workability tests have been  
 434 conducted in accordance with the criteria spelled out in EFNARC [5]. Table 6 summaries the

435 SCC workability performance. As indicated, all the test results have been evaluated against the  
 436 criteria in EFNARC [5]. In short, all the LWSCC mixes must pass fresh property assessment  
 437 tests, including filling ability (J-ring), passing ability (V-funnel and Slump flow) and  
 438 segregation resistance (visual segregation index and sieve stability).

439 **Table 6: EFNARC requirement**

Workability	Test	Class	Criteria
Filling ability	Slump Flow (mm)	SF1	550-650
		SF2	660-750
		SF3	760-850
	T500 (s)	VS1/VF1	$\leq 2$ V – Funnel $\leq 8$
		VS2/VF2	$\geq 2$ time(s) 9 – 25
Passing ability	Step height in J-ring (mm)	PA1	$S_j \leq 15$ (59 mm bar spacing)
		PA2	$S_j \leq 15$ (40 mm bar spacing)
	U-Box		0.8 - 0.1
			0 - 30
Segregation Resistance	Sieve segregation (%)	SR1	$\leq 20$
		SR2	$\leq 15$

440

441 As discussed in methodology section, fresh properties of LWSCC had to be assessed. The  
 442 filling ability was assessed using J-ring test while passing ability was assessed through V-  
 443 funnel and slump flow tests. Segregation resistance was assessed using visual segregation index  
 444 and sieve stability tests. Table 7 shows the fresh property test results. Further evaluation and  
 445 elaboration of these results will be done in the following section.

446

**Table 7: Summary of fresh properties**

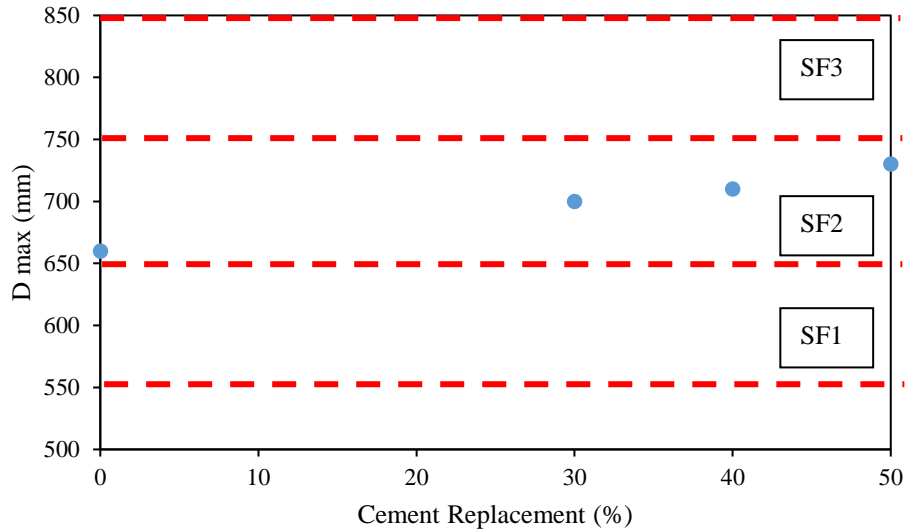
<b>Tests</b>	<b>Mixes</b>	<b>M0</b>	<b>M30</b>	<b>M40</b>	<b>M50</b>
<b>J-Ring</b>	<b>T<sub>500</sub> (s)</b>	10	9	8.4	7
	<b>Dm (mm)</b>	520	580	530	600
	<b>Block Step (mm)</b>	12.5	9.75	8.5	9.5
<b>Slump flow</b>	<b>T<sub>500</sub> (s)</b>	5.04	4.38	4.35	1.82
	<b>Dm (mm)</b>	665	700	710	730
<b>V-funnel</b>	<b>T<sub>10s</sub> (s)</b>	15	14	13	13
	<b>T<sub>5min</sub> (s)</b>	24	18	18	17
<b>Sieve segregation</b>	<b>Sieved Portion (%)</b>	6.28	6.84	5.95	4.8
<b>Visual Index</b>	<b>Index</b>	1	1	1	1

448

#### 449 **4.1.1 Filling Ability**

450 Filling ability is meant to measure the ability of fresh LWSCC to flow and fill formwork under  
 451 self-weight without the need of external vibration. In this research, assessment of flow ability  
 452 of LWSCC have been done by carrying out slump flow and V-funnel tests.

453 All the LWSCC mix designs in this research have achieved the slump flow spread of 660-  
 454 730mm as shown in Figure 5. These values were within the range 550-850mm of European  
 455 guidelines [6]. In particular, they fell within class SF2 of European Guideline with range of  
 456 650-750mm. SCC which fulfils Class SF2 requirement is meant for use in vertical structural  
 457 components such as walls and columns. The maximum spread of LWSCC tends to increase  
 458 with higher level fly ash replacement. It is a well-established fact that the use of FA in SCC  
 459 can reduce the water demand required to achieve a given workability. Meanwhile,  
 460 incorporation of fly ash can reduce the need of superplasticiser at constant w/b ratio to obtain  
 461 a given slump flow. Similar outcomes were observed by Yahia et al. [89] and Ramanathan et  
 462 al. [68].



463

464

**Figure 5: Comparison of maximum slump spread**

465

$T_{500}$  and V-funnel flow times are used to assess the viscosity and stability of SCC respectively.

466

Figure 6 and Figure 7 present  $T_{500}$  and V-funnel flow times of all mixes respectively. A low

467

values of  $T_{500}$  and V-funnel flow time indicate that the fresh concrete possesses low plastic

468

viscosity and therefore it has faster filling rate. The time to spread 500mm for four mixes fell

469

in the range of 1.82 – 5.04s. The control mix, 30% and 40% were classified as class VS2 as the

470

flow time was more than 2s while mix 50% was classified as class VS1.  $T_{500}$  was found to

471

decrease with the increasing content of fly ash. V-funnel test was carried out in two conditions,

472

which were when funnel trap door was opened 10 seconds and 5 minutes after filling with

473

LWSCC respectively. V-funnel time was in the range of 13 -15s for  $T_{10s}$  and 17-25s for  $T_{5min}$ .

474

Since  $T_{10s}$  was more than 8s, all the LWSCC were classified as Class VF2 of European

475

guidelines. The inverted cone shape of V-funnel restricts concrete flow and the prolonged flow

476

time can give an indication of fresh concrete blocking tendency. The control mix was found to

477

have the highest v-funnel flow time.  $T_{10s}$  tended to decrease with the increase of fly ash

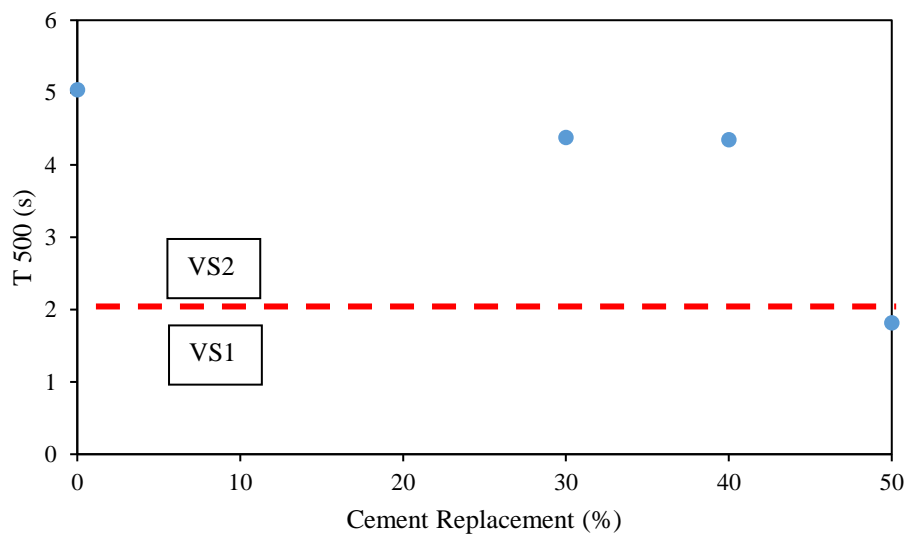
478

replacement. Similar trend was found for  $T_{5min}$ . This is depicted in Figure 7. The relationship

479

between  $T_{500}$  and V-funnel flow time is presented in Figure 8. Two mixes fall in VS2/VF2

480 category. According to EGSCC [6], the mix that falls within VS2/VF2 region gives rise to good  
481 filling rate. The mixes which fall within this region can experience thixotropic effect that can  
482 help to reduce formwork pressure. However, the resultant hardened concrete may experience  
483 blow hole finishing surface. Slump flow and flow times depend highly on replacement level of  
484 fly ash. As such, fly ash is found to be able to improve filling ability of LWSCC. The capability  
485 of fly ash to improve workability of LWSCC is derived from the round shape and smooth  
486 nature of fly ash particles which induce ball bearing effect. Replacing cement partially with fly  
487 ash can result in higher volume of paste and this eases friction at the interface between fine  
488 aggregate and paste. Consequently, cohesiveness and plasticity of concrete improve. Hence,  
489 the improved concrete workability is achieved [68]. In short, incorporating fly ash as partial  
490 binder content in LWSCC with OPS as coarse aggregates has been proven, by good filling  
491 ability results, to have similar performance to conventional SCC.

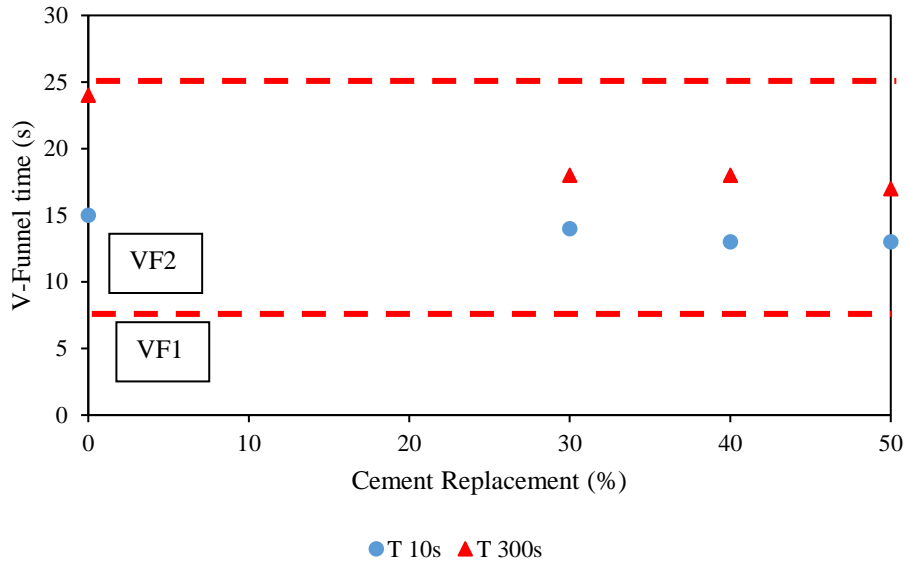


492

493

**Figure 6: Comparison of slump flow time**

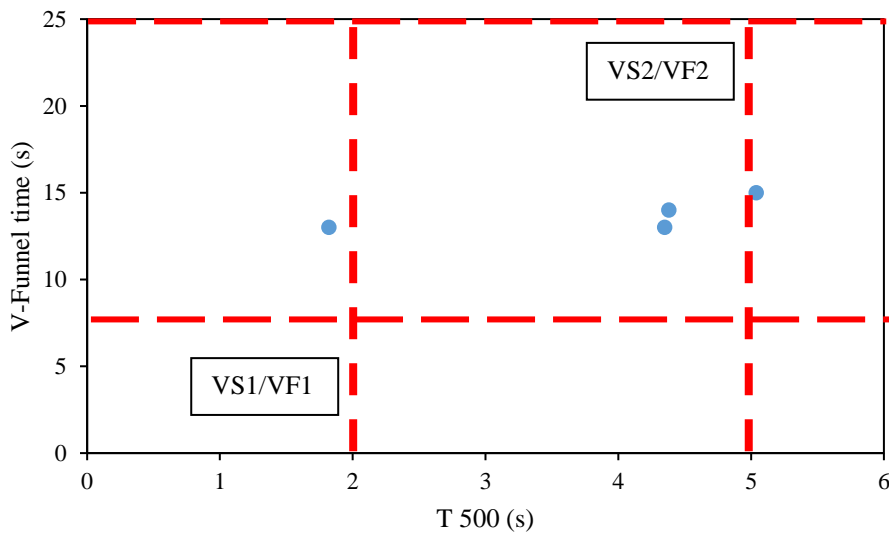
494



495

496

**Figure 7: V-funnel time comparison**



497

498

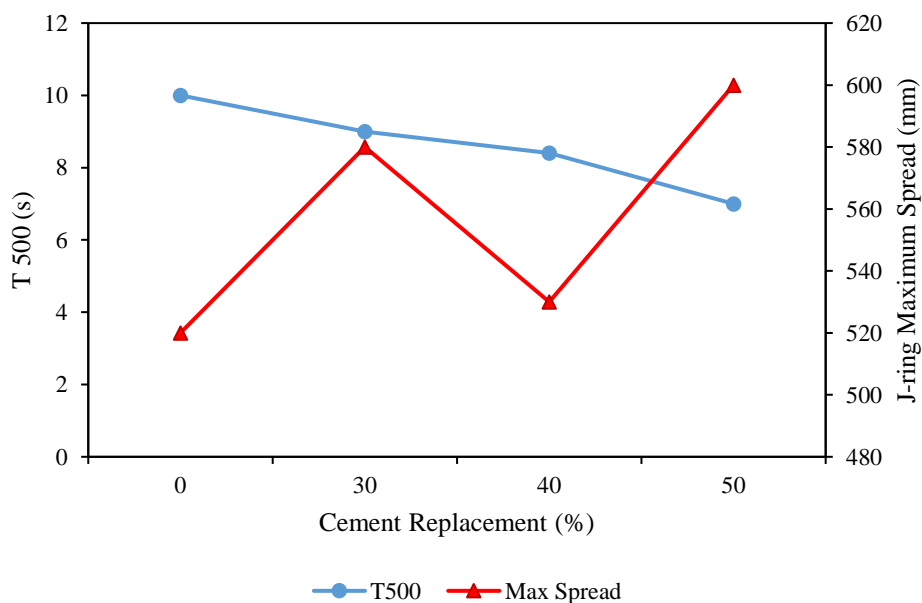
**Figure 8: Viscosity class variation with T500 and V-funnel flow time**

499

#### 500 4.1.2 Passing Ability

501 Passing ability is assessed to determine the capability of a fresh LWSCC to pass through narrow  
 502 openings in confined space such as heavily steel reinforced area, with no segregation and loss  
 503 of its uniform consistency or without blockage in the confined space.

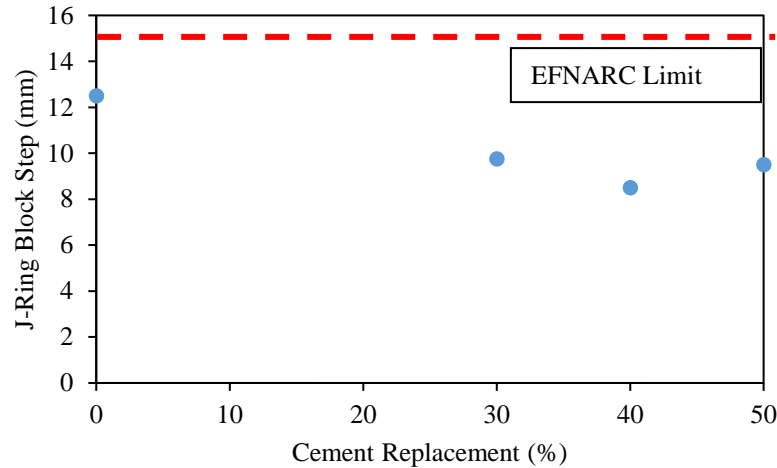
504 Passing ability of LWSCC was determined by conducting J-ring test. Three key parameters of  
 505 J-ring test are indicated as  $T_{500}$  (time to spread 500mm diameter),  $D_m$  (maximum spread) and  
 506 block step. The main concern is block step value which is the difference in concrete height  
 507 between inside and outside of J-ring bars. Block step of 15mm is within acceptable range of  
 508 EGSCC [6]. From Table 7, the time used to spread 500mm diameter is in the range of 7s to 10s  
 509 while the maximum spread is ranging from 520mm to 600mm. These values are shown in  
 510 Figure 9. The time taken to spread 500mm decreased with higher replacement of fly ash in j-  
 511 ring test. The block step is in the range of 9.5mm to 12.5mm. Higher block step values indicate  
 512 higher viscosity whereby there is higher blockage tendency of coarse aggregate when the fresh  
 513 SCC flows through steel bars. Figure 10 shows block step height of three SCC samples. It is  
 514 noted that block step height reduces when the fly ash replacement is increased from 0 to 40%.  
 515 However, the block step height increases when fly ash replacement is increased from 40% to  
 516 50%. This signifies that passing ability of LWSCC improves with replacement of fly ash up to  
 517 40%. In short, replacement of fly ash in LWSCC offers better passing ability up to an optimum  
 518 point.



519

520

**Figure 9: T 500 and max spread comparison**



521

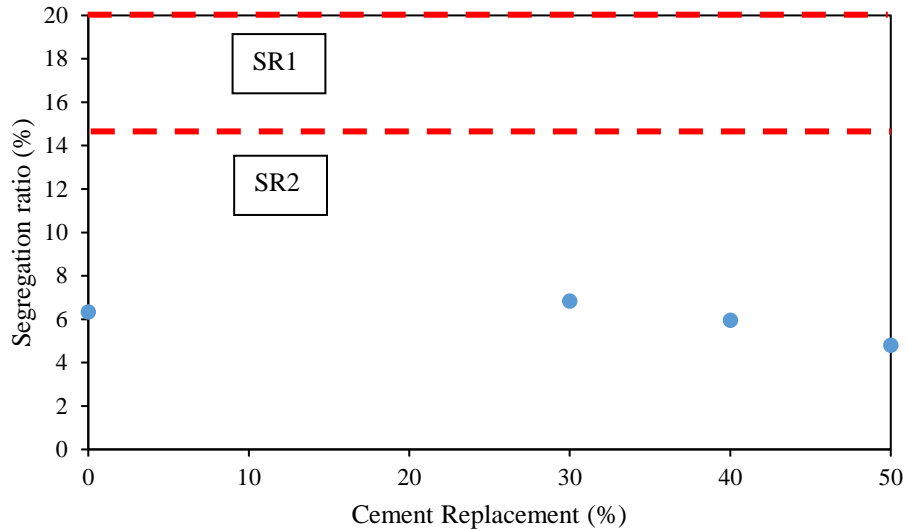
522

**Figure 10: Comparison of j-ring block step height**

523 **4.1.3 Segregation Resistance**

524 Segregation resistance is assessed to ensure LWSCC maintains its homogeneity which means  
 525 it does not bleed and its aggregates do not segregate during concreting and transportation  
 526 processes. Sieve segregation and visual indexing were used to assess LWSCC segregation  
 527 resistance.

528 Percentage of concrete mix passing through 5mm sieve is expressed as segregation ratio. Figure  
 529 11 depicts the comparison of segregation of LWSCC at different levels of fly ash replacement.  
 530 Smaller segregation ratio indicates that LWSCC has better segregation resistance. From the  
 531 figure, all the four concrete mixes achieved segregation ratio of less than 15%, which meant  
 532 that their segregation resistance fell within class SR2. Concrete mixes within Class SR2 can be  
 533 utilized in tall vertical structures. All the LWSCC can be considered as quite consistent in  
 534 eschewing segregation and bleeding. The binder content, w/b ratio, amount of SP and  
 535 aggregates content were proportioned carefully to produce mixes with constant fresh concrete  
 536 properties. By comparing the segregation ratio of 30% mix with the control, 30% mix resulted  
 537 in slightly poorer sieve segregation. However, as fly ash content increased, the segregation  
 538 resistance improved up to 50% of fly ash replacement.

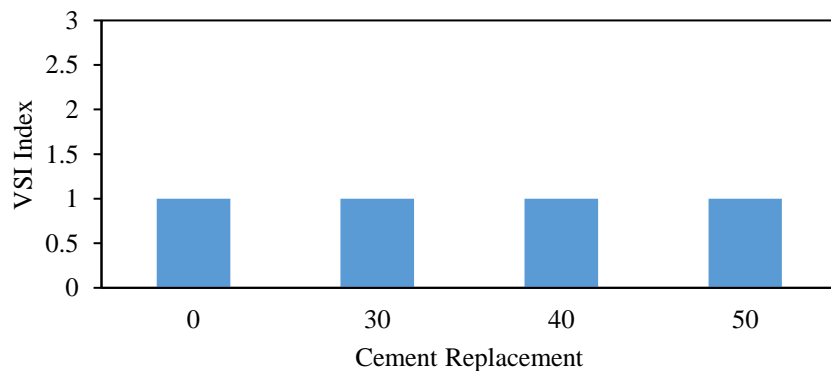


539

540

**Figure 11: Comparison of segregation ratio**

541 In this study, visual segregation indices were taken straight after the slump flow tests. These  
 542 indices were recorded based on the presence of mortar halo and aggregates piling up at the  
 543 centre of spread, as well as any separation of aggregates and mortar at the edge. Figure 12  
 544 shows the VSI indices of all four LWSCC mix designs. All the mix designs show the VSI index  
 545 of 1.0, which indicated no mortar halo or aggregate piled up at the centre and also, minor  
 546 evidence of air popping on the surface of LWSCC spread. Typical slump flow spread is shown  
 547 in Figure 13. These VSI indices have agreed with the results of sieve segregation and thus  
 548 demonstrated satisfactory segregation resistance of the mix.



549

550

**Figure 12: Comparison of VSI index**



551

552

**Figure 13: Typical slump flow appearance**

553 These experiments have shown that the OPS based SCC satisfies the requirement of the fresh  
554 state properties of SCC such as filling ability, passing ability and segregation resistance. As  
555 such, OPS is considered a potential material which can be used to replace normal aggregate in  
556 manufacturing SCC.

## 557 **4.2 Hardened Properties under Room Temperature**

### 558 **4.2.1 Density**

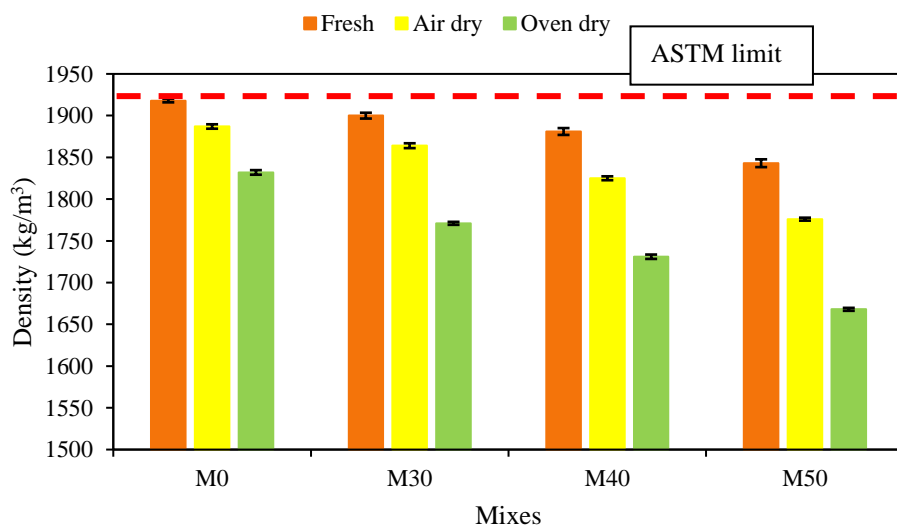
559 The density for all LWSCC mixes under fresh, air dry and oven dry conditions is shown in  
560 Table 8. Overall, all the mixes have achieved density in the range of 1800 kg/m<sup>3</sup> to 2000kg/m<sup>3</sup>  
561 for fresh density. The air dry density is about 40-70 kg/m<sup>3</sup> lower than fresh density while oven  
562 dry density is 125-175 kg/m<sup>3</sup> lower than fresh density. The comparison of density between  
563 mixes under different conditions is illustrated in **Error! Reference source not found. Error!**  
564 **Reference source not found.** The density of control mix does not fall within the range of  
565 1120-1920 kg/m<sup>3</sup> which is specified by ASTM C330 as light weight concrete. Nevertheless,  
566 the control mix has achieved weight some 17% lighter compared to normal granite based  
567 concrete. It is noted that the density of concrete reduces with increasing replacement level of

568 fly ash in the binder content of concrete. This reduction of density is due to the lower specific  
 569 gravity of fly ash compared to cement. Similar trend of results was reported by Shafigh et al.  
 570 [50] with fly ash substitution up to 70% for normally vibrated OPS based concrete. Reduced  
 571 density of concrete can lead to better economic design of structure as dead load of structure is  
 572 decreased significantly.

573 **Table 8: Concrete density**

Mix	Density (kg/m <sup>3</sup> )		
	Demoulded	Air dry	Oven dry
M0	1918	1887	1832
M30	1900	1864	1771
M40	1881	1825	1731
M50	1843	1776	1668

574



575

576 **Figure 14: Comparison of mixes density**

#### 577 4.2.2 Compressive Strength

578 Concrete compressive strength is regarded as the most important property which determines  
 579 structural performance of the material. The compressive strength of LWSCC mixes at 7, 28  
 580 and 90 day age is summarized in Table 9. The compressive strengths for all mixes fall within

581 the range of 13-27MPa at 7 day, 18-39MPa at 28 day and 24-41MPa at 90 day. Development  
582 of compressive strength for all LWSCC mixes is illustrated in Figure 15**Error! Reference**  
583 **source not found.** The compressive strength improved with increasing age from 7 days to 90  
584 days. Test results show that control mix attained the highest compressive strength among all  
585 four mixes. When fly ash substitution level was raised from 30% to 50%, the compressive  
586 strength decreased drastically. From Figure 15**Error! Reference source not found.**, it is  
587 observed that the mixes that contain fly ash experienced slower rate of strength gain compared  
588 to control mix at early age. At latter age, mixes that contained fly ash still experienced  
589 significant strength gain while control mix did not. Mix M30 achieved comparable strength to  
590 control mix M0 at 90-day age. Similar trends were also observed in the studies of normally  
591 vibrated OPS based concrete done by Kupaei et al. [91] and Shafigh et al. [50]. These can be  
592 explained that the pozzolanic reactions in concrete have slowed down due to low calcium  
593 content in Class F fly ash, leading to significant delay in early strength gain. This effect is more  
594 significant when there is higher level of fly ash replacement.

595 For failure mode of LWSCC samples, it is observed that fracture occurred through the LWA  
596 particles. This observation indicates that aggregates are feeble within LWSCC concrete matrix.  
597 In the study of normally vibrated OPS concrete, Okpala [23] claimed that failure of OPS  
598 concrete was governed by the breakdown of bond between aggregates and cement mortar.  
599 Mannan et al. [30] also attributed OPS concrete failure to lack of adhesion between OPS  
600 aggregate and cement paste. Floyd et al. [87] reported similar observation in the study of  
601 expanded clay as LWA in LWSCC. Lotfy et al. [92] also reported that aggregate fracture was  
602 observed in failed sample after compression test for LWSCC. Thus, stiffness of LWA plays a  
603 critical role in contributing to strength of LWSCC. In other words, cement mortar in LWSCC  
604 is typically stronger than LWA and contributes the most strength [15]. It is thus concluded that

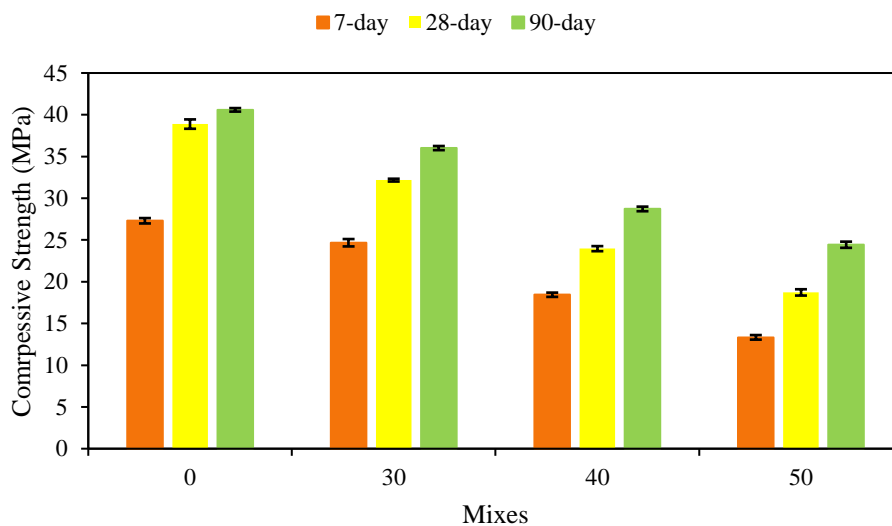
605 the individual strength of LWA is important in contributing to the compressive strength of  
 606 LWSCC.

607

608 **Table 9: Concrete compressive strength at different age**

Mix	Compressive Strength (MPa)		
	7 days	28 days	90 days
M0	27.30	38.88	40.59
M30	24.67	32.17	36.01
M40	18.44	23.96	28.72
M50	13.34	18.72	24.43

609



610

611 **Figure 15: LWSCC compressive strength development with time**

612 **4.2.3 Splitting Tensile Strength**

613 Splitting tensile strength is a material property which can be utilized to assess the diagonal  
 614 tension resistance of LWSCC structure. The splitting tensile strength for OPS based SCC mixes  
 615 at 7, 28 and 90 day is summarized in Table 10. The splitting tensile strength varies from 1.2-  
 616 2.2MPa at 7 day, 1.6-2.8MPa at 28 day and 2-2.8MPa at 90 day. ASTM C330 has specified a  
 617 minimum value of 2MPa splitting tensile strength for LWA concrete. All the mixes except M50

618 have achieved 2MPa and above strengths at 28 day. Development of LWSCC splitting tensile  
 619 strength is shown in Figure 16 **Error! Reference source not found.** Splitting tensile strength  
 620 is observed to increase as concrete ages. Similar to compressive strength, slower rate gain in  
 621 splitting tensile strength is noted on concrete that contains fly ash. This effect is more  
 622 significant at higher level of fly ash substitution. In short, increase in fly ash content decreases  
 623 concrete splitting tensile strength.

624 **Table 10: Concrete splitting tensile strength at different age**

Mix	Splitting Tensile Strength (MPa)		
	7 days	28 days	90 days
M0	2.19	2.82	2.84
M30	2.09	2.54	2.75
M40	1.62	2.05	2.33
M50	1.20	1.62	2.07

625  
 626 Similar to granite based concrete, splitting tensile strength of OPS based SCC can also be  
 627 correlated to its compressive strength. Relationship between compressive strength and splitting  
 628 tensile strength is shown in Figure 17. The splitting tensile strength is noted to increase with  
 629 increasing value of compressive strength. As shown in the experimental results, splitting tensile  
 630 strength is about 7.2- 8.6% of compressive strength which is within the range of normally  
 631 vibrated OPS based concrete reported by several researchers. Mahmud et al. [93] reported  
 632 values of 6-10% of their OPS based concrete compressive strength. Values of 6.7-8.1% were  
 633 also reported by Shafigh et al. [36] based on their extensive research on splitting tensile strength.  
 634 A recent study on normally vibrated OPS based concrete with fly ash replacement by Shafigh  
 635 et al. [50] shows the values of 5-7%.

636 As illustrated in Figure 18, the ratio of splitting tensile strength to compressive strength  
 637 decreases when the compressive strength of LWSCC increases. The trends agree with the  
 638 findings of Shafigh et al. [36] for normally vibrated OPS based concrete. This trend shows that

639 OPS based SCC exhibits similar properties to normally vibrated OPS based concrete. The  
640 correlation between splitting tensile strength and compressive strength of concrete from various  
641 researchers are shown in Table 11. These equations are used to predict the splitting tensile  
642 strength and plotted in Figure 19 for comparison purpose. The vertical axis is expressed as ratio  
643 of calculated value to experimental value. It is noted that the predicted values from equation of  
644 Farahani et al. [48] are closest to the experimental results. The proposed equation by Felekoğlu  
645 et al. [94] overestimates the splitting tensile strength as the equation is meant for granite based  
646 SCC. Contradictory to Felekoğlu et al. [94], the equation proposed by Lotfy et al. [92]  
647 underestimates the splitting tensile strength as this equation is actually proposed for furnace  
648 slag, expanded clay and expanded shale based SCC. These findings demonstrated that the  
649 splitting tensile strength of concrete is highly dependent on the type of aggregates used. An  
650 equation for correlation of compressive strength with tensile splitting strength for OPS based  
651 SCC, which has been proposed in the present study is shown as Eq. (13) below:

$$f_t = 0.1803f_{cu}^{0.7573} \quad (R^2 = 0.9896) \quad (13)$$

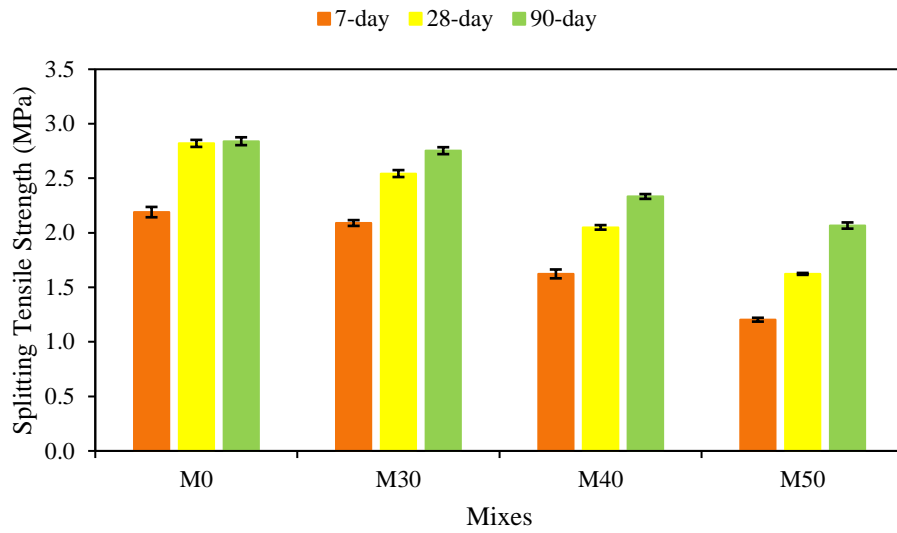
652 where  $f_t$  is splitting tensile strength and  $f_{cu}$  is ultimate cube strength of concrete.

653 **Table 11: Splitting tensile strength equations from various researchers**

Researchers	Equation	Description	
Shafigh et al. [31]	$0.2\sqrt[3]{f_c^2}$	Normally vibrated OPS concrete containing uncrushed OPS with compressive strength ranging from 17MPa to 37MPa	(14)
Shafigh et al. [36]	$0.4887\sqrt{f_c}$	Normally vibrated OPS concrete containing crushed OPS	(15)
Shafigh et al. [52]	$0.23f_c^{0.64}$	Normally vibrated OPS concrete containing crushed OPS and 10-50% fly ash	(16)
Farahani et al. [48]	$0.146f_c^{0.835}$	Normally vibrated OPS concrete containing crushed and blended binder of OPC, RHA and FA	(17)

Lotfy et al. [92]	$0.177f_c^{1.33}$	Lightweight self-compacting concrete containing furnace slag, expanded clay and expanded shale as LWA	(18)
Felekoğlu et al. [94]	$0.43f_c^{0.6}$	Self-compacting concrete with granite as aggregates	(19)

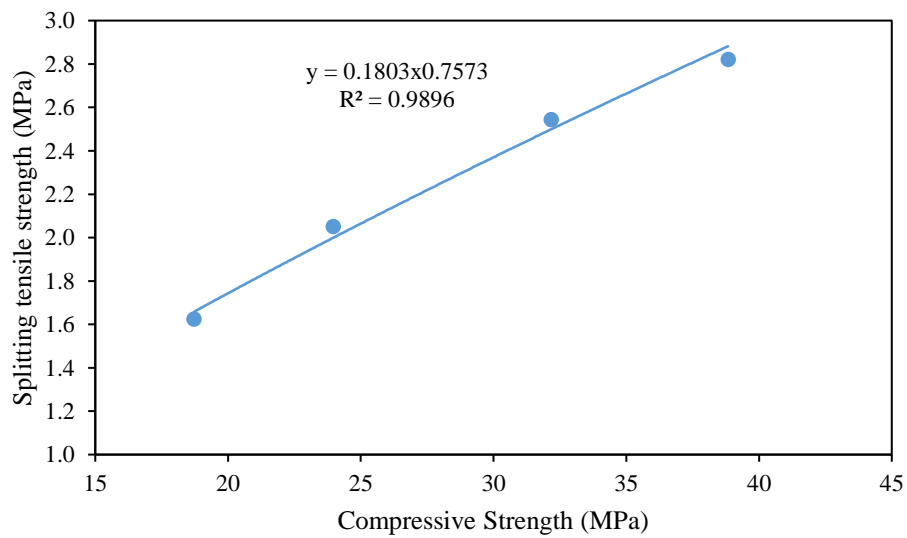
654



655

656

**Figure 16: LWSCC splitting tensile strength development with time**

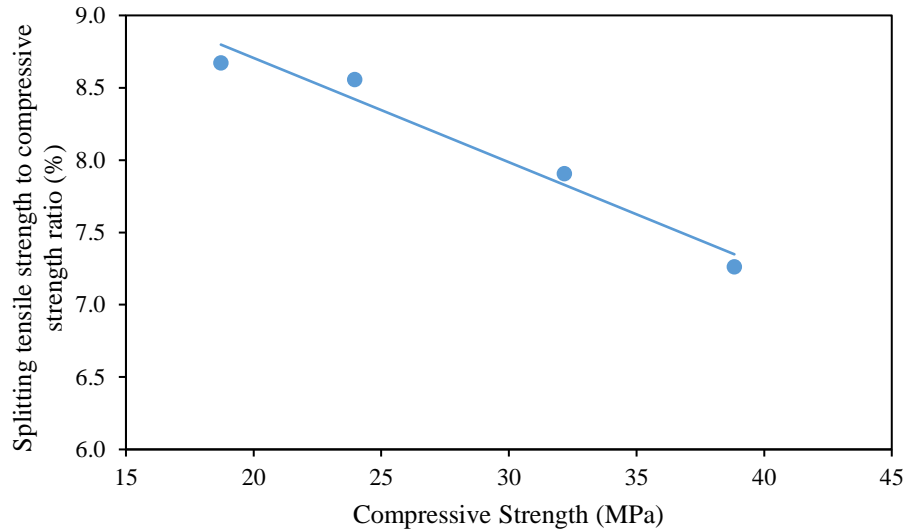


657

658

**Figure 17: Correlation of LWSCC compressive strength to splitting tensile strength**

659



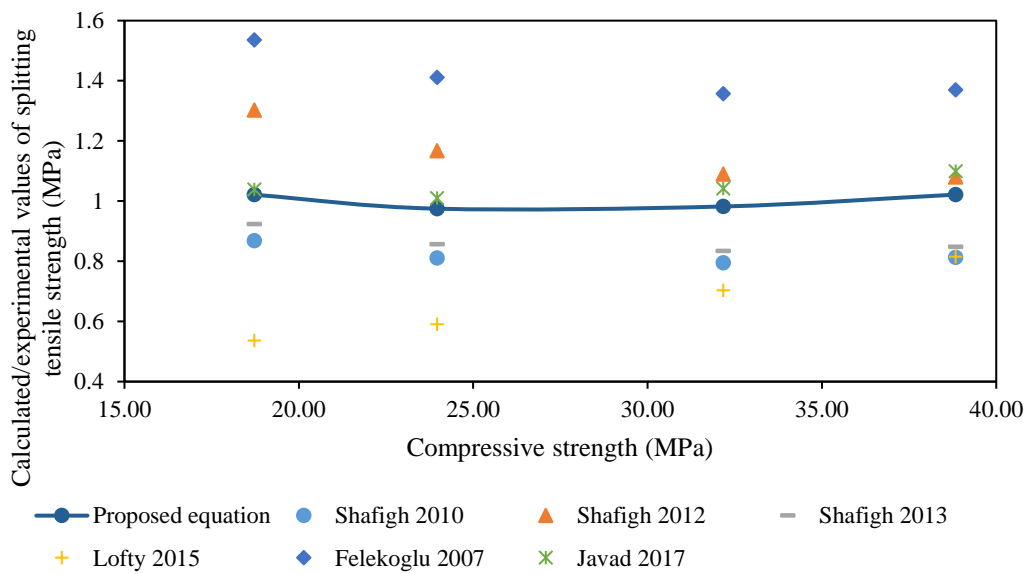
660

661

**Figure 18: Correlation of compressive strength to ratio of splitting tensile to compressive strength**

662

663



664

665

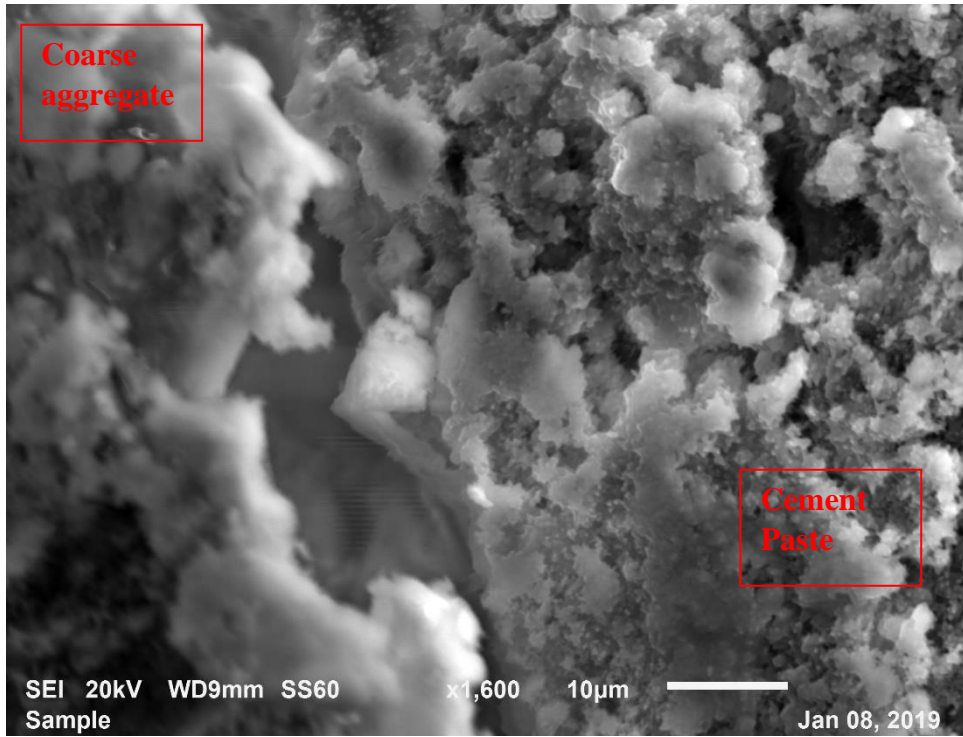
**Figure 19: Relationship between 28-day compressive strength and calculated splitting tensile strength**

666

#### 667 4.2.4 SEM Analysis

668 The interfacial transition zones (ITZ) between binder and aggregates have been investigated  
669 by using SEM technique. This is to study the bonding characteristics between cement paste and  
670 aggregates of chosen LWSCC samples. The SEM images for Mix M0 at 28 day and 90 day are  
671 shown in Figure 20 and Figure 21 respectively. As shown in these two images, cement paste  
672 has considerably seeped into the surface pores of OPS aggregate in the interfacial transition  
673 zone (ITZ) to form interlocking structure. The rough surfaces and micro-pores of OPS provide  
674 bigger surface area to receive cement paste. Moreover, high workability of LWSCC has  
675 ensured homogeneity of hardened concrete. This can enhance the interlocking bond between  
676 cement paste and aggregates.

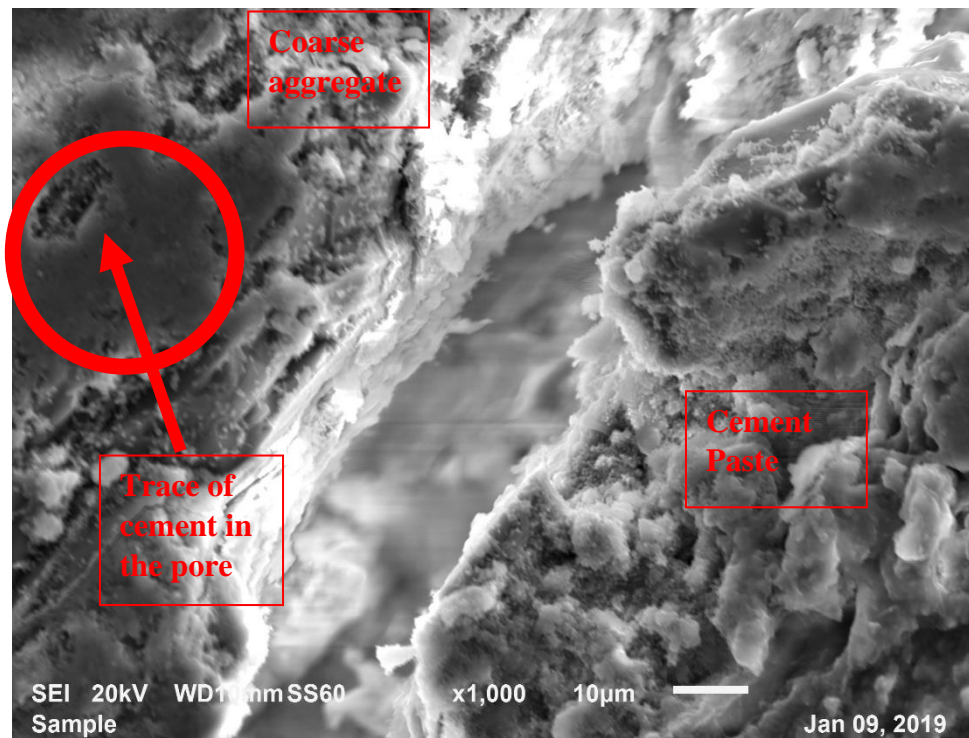
677 The SEM images for Mix M50 at 28 day and 90 day are shown in Figure 22 and Figure 23. It  
678 can be noticed in Figure 22 that smooth spherical fly ash particles are still present, which shows  
679 that fly ash is still in the early stage of hydration as its initial shape is spherical. As such, the  
680 pozzolanic reactions of fly ash and cement are not complete in the initial phase of hydration  
681 [95]. As concrete ages, decomposition of the spherical shape of fly ash gradually takes. Figure  
682 23 indicates that the round-shaped fly ash particles are not as easily noticeable as the material  
683 is at the age of 90 days. These observations prove that the rate of hydration in concrete is  
684 reduced by fly ash. It is also noted that the aggregate surface is full of binder particles. The  
685 results accorded well with the works of Alengaram et al. [49] that finer supplementary  
686 cementitious material could enhance the ITZ to improve mechanical bonding.



687

688

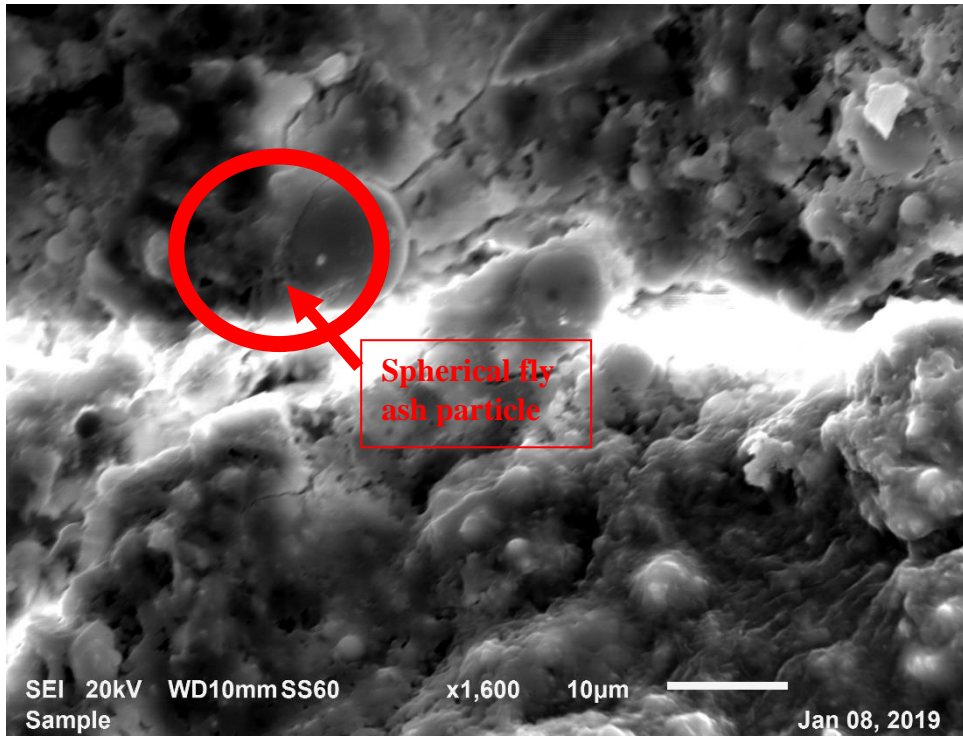
**Figure 20: SEM image of ITZ of M0 at 28 day**



689

690

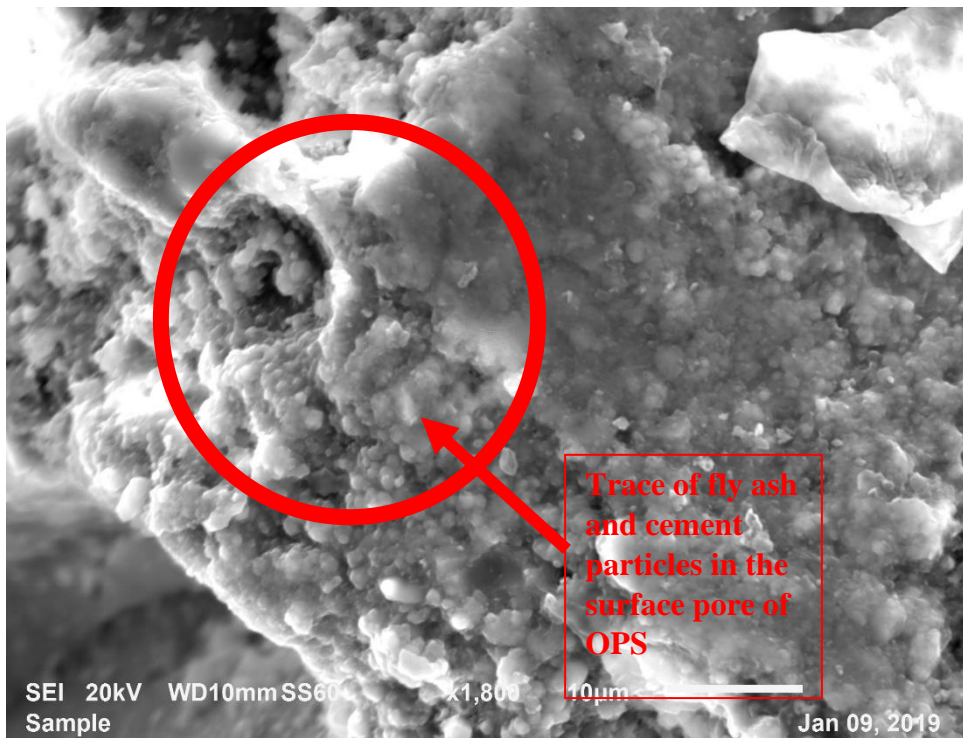
**Figure 21: SEM image of ITZ of M0 at 90 day**



691

Figure 22: SEM image of ITZ of M50 at 28 day

692



693

Figure 23: SEM image of aggregate part at ITZ of M50 at 90 day

694

#### 695 4.2.5 Water Absorption

696 Concrete water absorption values of all four mix designs are presented in Table 12 and  
697 illustrated in Figure 24**Error! Reference source not found.** The water absorption values for  
698 all mixes were 6.1-7.33% at 28 day and 4.47- 5.07% at 90 day. At 28-day age, control LWSCC  
699 mix had the lowest water absorption value among the four mixes. It is noticed that increasing  
700 the substitution of fly ash in OPS based LWSCC increases water absorption at earlier age. This  
701 is because increasing of class F fly ash content in concrete reduces the hydration process at  
702 earlier age. At earlier age, the hydration process in high fly ash content concrete is not complete  
703 and capillary pores still exist which are permeable, resulting in higher water absorption [96].  
704 Several researchers [50, 52] have demonstrated that the water absorption of normally vibrated  
705 OPS increases with increasing of fly ash content. The study of Shafigh et al. [52] shows that  
706 the water absorption of normally vibrated OPS concrete increases from 5.5% to 6.6%, 7% and  
707 9.8% when fly ash content is increased from 0% to 10%, 30% and 50% respectively.

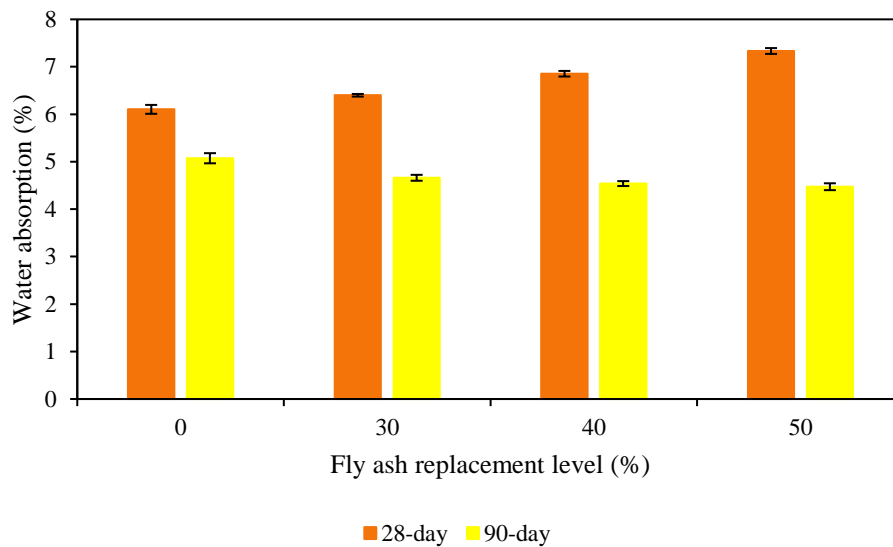
708 At 90-day age, concrete of all the four mixes shows reduction in water absorption. It is observed  
709 that the water absorption at 90 day reduced by 17%, 27%, 34% and 39% for M0, M30, M40  
710 and M50 respectively when compared to 28 day. At 90-day age, for concrete incorporated with  
711 fly ash, the voids between particles of materials were filled with fly ash at higher percentage  
712 and thus the porosity of concrete was reduced. The texture and size of the fly ash particles are  
713 able to minimize the voids in between particles [97]. The results show that water absorption  
714 of LWSCC decreases with age especially those with higher fly ash content. This is because the  
715 interconnectivity of the pores in concrete structure is reduced by fly ash as it uses  $\text{Ca(OH)}_2$   
716 from the cement and induces secondary calcium silicate to hydrate at later age [98]. However,  
717 the total porosity of concrete is increased with the incorporation of fly ash. Nevertheless, the  
718 ratio pore refinement to “pore size” is reduced [99].

719 Generally, all the concrete mixes exhibited water absorption of less than 8% at all ages. Neville  
 720 [18] stated good concrete must possess the water absorption value of less than 10%, the result  
 721 of which can be determined from immersed water absorption test.

722 **Table 12: Water absorption value of OPS based LWSCC**

LWSCC Mix	Water Absorption (%)	
	28-day	90-day
M0	6.10	5.07
M30	6.40	4.66
M40	6.85	4.54
M50	7.33	4.47

723



724

725 **Figure 24: Water absorption of OPS based LWSCC**

726 **5.0 Conclusion**

727 LWSCC control mix design has been successfully derived in this experimental research.  
 728 Together with thorough investigation conducted on fresh and hardened properties of control  
 729 LWSCC mix as well as the concrete mixes incorporated with various proportions of fly ash  
 730 replacement to the control, the conclusions can be drawn as below:

- 731 1. LWSCC can be produced by using OPS as full replacement to normal weight aggregates  
732 (NWA), as well as with partial fly ash replacement, and the resultant concretes have  
733 satisfactorily achieved fresh state properties in respect of passing ability, filling ability and  
734 segregation resistance.
- 735 2. OPS-aggregate based LWSCC achieves satisfactory slump flow spread in the range of 665-  
736 730mm.
- 737 3. Satisfactory V-funnel flow time of less than 25s which meets specification in the European  
738 Guidelines has been achieved.
- 739 4. OPS based LWSCC has achieved good passing ability with the block step in the range of  
740 8-15mm.
- 741 5. Excellent segregation resistance with value in the range of 4-7% has been achieved.
- 742 6. All the fresh concrete properties of SCC using OPS as aggregates improve with partial  
743 replacement of fly ash.
- 744 7. The density of OPS based SCC is found to be 15%-23% lower than normal concrete.  
745 Substitution of Ordinary Portland Cement with fly ash also reduces the concrete density.
- 746 8. The compressive strength of LWSCC is in the range of 18 to 38MPa at 28-day age. The  
747 compressive strength of LWSCC mix with fly ash replacement increases with curing age.
- 748 9. The splitting tensile strength of LWSCC is found to be in the range of 1.6-2.8MPa at 28-  
749 day-age. Splitting tensile strength falls in the range 7.2- 8.6% of its compressive strength.  
750 Its strength also improves with curing age.
- 751 10. As evidenced in SEM tests, cement paste has seeped into the pores of OPS aggregates  
752 giving rise to good bonding in the ITZ.
- 753 11. All the OPS based LWSCC exhibits water absorption of less than 8% at all ages. Water  
754 absorption of LWSCC decreases with age and, the decrease is more conspicuous for  
755 concrete with higher content of fly ash.

756 **Acknowledgement**

757 The authors would like to acknowledge full research funding provided by Curtin Malaysia  
758 Research Institute (CMRI 6020) and laboratory support provided by Curtin University  
759 Malaysia.

760 **Competing of Interests**

761 The authors declare no competing interests.

762 **References**

- 763 [1] F.U.A. Shaikh, S. Luhar, H.Ş. Arel, I. Luhar, Performance evaluation of Ultrahigh  
764 performance fibre reinforced concrete–A review, *Construction and Building Materials* 232  
765 (2020) 117152.
- 766 [2] H. Okamura, M. Ouchi, Self-compacting high performance concrete, *Progress in Structural*  
767 *Engineering and Materials* 1(4) (1998) 378-383.
- 768 [3] S. Ghorbani, S. Sharifi, H. Rokhsarpour, S. Shoja, M. Gholizadeh, M.A.D. Rahmatabad, J.  
769 de Brito, Effect of magnetized mixing water on the fresh and hardened state properties of steel  
770 fibre reinforced self-compacting concrete, *Construction and Building Materials* 248 (2020)  
771 118660.
- 772 [4] E. Güneyisi, Y.R. Atewi, M.F. Hasan, Fresh and rheological properties of glass fiber  
773 reinforced self-compacting concrete with nanosilica and fly ash blended, *Construction and*  
774 *Building Materials* 211 (2019) 349-362.
- 775 [5] A. EFNARC, *Specification and Guidelines for Self-Compacting Concrete*, Surrey, UK:  
776 EFNARC, Association House, 2002.
- 777 [6] EGSCC, *The European Guidelines for Self-Compacting Concrete*, (2005).
- 778 [7] ACI-237, 237. “, ACI 237R-07–Self-Consolidating Concrete”. American Concrete Institute  
779 (2007).
- 780 [8] U.J. Alengaram, B.A. Al Muhit, M.Z. bin Jumaat, Utilization of oil palm kernel shell as  
781 lightweight aggregate in concrete–a review, *Construction and Building Materials* 38 (2013)  
782 161-172.
- 783 [9] İ.B. Topçu, T. Uygunoğlu, Effect of aggregate type on properties of hardened self-  
784 consolidating lightweight concrete (SCLC), *Construction and Building Materials* 24(7) (2010)  
785 1286-1295.
- 786 [10] P.K. Mehta, H. Meryman, Tools for reducing carbon emissions due to cement  
787 consumption, *Structure* 1(1) (2009) 11-15.
- 788 [11] E. Aprianti, A huge number of artificial waste material can be supplementary cementitious  
789 material (SCM) for concrete production–a review part II, *Journal of Cleaner Production* 142  
790 (2017) 4178-4194.
- 791 [12] M. Etxeberria, E. Vázquez, A. Marí, M. Barra, Influence of amount of recycled coarse  
792 aggregates and production process on properties of recycled aggregate concrete, *Cement and*  
793 *concrete research* 37(5) (2007) 735-742.
- 794 [13] J. Xiao, J. Li, C. Zhang, Mechanical properties of recycled aggregate concrete under  
795 uniaxial loading, *Cement and concrete research* 35(6) (2005) 1187-1194.

- 796 [14] Z.H. Duan, C.S. Poon, Properties of recycled aggregate concrete made with recycled  
797 aggregates with different amounts of old adhered mortars, *Materials & Design* 58 (2014) 19-  
798 29.
- 799 [15] T.M. Grabois, G.C. Cordeiro, R.D. Toledo Filho, Fresh and hardened-state properties of  
800 self-compacting lightweight concrete reinforced with steel fibers, *Construction and Building*  
801 *Materials* 104 (2016) 284-292.
- 802 [16] C.-L. Hwang, M.-F. Hung, Durability design and performance of self-consolidating  
803 lightweight concrete, *Construction and Building Materials* 19(8) (2005) 619-626.
- 804 [17] F. Tajra, M. Abd Elrahman, C. Lehmann, D. Stephan, Properties of lightweight concrete  
805 made with core-shell structured lightweight aggregate, *Construction and Building Materials*  
806 205 (2019) 39-51.
- 807 [18] A. Neville, *Properties of concrete CTP-VVP*, Malaysia, 2008.
- 808 [19] ACI-213, *Guide for Structural Lightweight-aggregate Concrete*, American Concrete  
809 Institute, 2003.
- 810 [20] M. Aslam, P. Shafigh, M.Z. Jumaat, Oil-palm by-products as lightweight aggregate in  
811 concrete mixture: a review, *Journal of Cleaner Production* 126 (2016) 56-73.
- 812 [21] T. Ting, M. Rahman, H. Lau, M. Ting, Recent development and perspective of lightweight  
813 aggregates based self-compacting concrete, *Construction and Building Materials* 201 (2019)  
814 763-777.
- 815 [22] H. Mahmud, Mix design and mechanical properties of oil palm shell lightweight aggregate  
816 concrete: a review, *International journal of the physical sciences* 5(14) (2010).
- 817 [23] D. Okpala, Palm kernel shell as a lightweight aggregate in concrete, *Building and*  
818 *environment* 25(4) (1990) 291-296.
- 819 [24] F.O. Okafor, Palm kernel shell as a lightweight aggregate for concrete, *Cement and*  
820 *Concrete Research* 18(6) (1988) 901-910.
- 821 [25] T. Pantzaris, A. Mohd Jaaffar, Properties and utilization of palm kernel oil, *Palmas*  
822 *(Colombia)* (2002).
- 823 [26] M. Tripathi, J. Sahu, P. Ganesan, P. Monash, T. Dey, Effect of microwave frequency on  
824 dielectric properties of oil palm shell (OPS) and OPS char synthesized by microwave pyrolysis  
825 of OPS, *Journal of Analytical and Applied Pyrolysis* 112 (2015) 306-312.
- 826 [27] K.A. Mujedu, M.A. Ab-Kadir, M. Ismail, A review on self-compacting concrete  
827 incorporating palm oil fuel ash as a cement replacement, *Construction and Building Materials*  
828 258 (2020) 119541.
- 829 [28] B.H. Nagaratnam, M.E. Rahman, A.K. Mirasa, M.A. Mannan, S.O. Lame, Workability  
830 and heat of hydration of self-compacting concrete incorporating agro-industrial waste, *Journal*  
831 *of Cleaner Production* 112 (2016) 882-894.
- 832 [29] H. Rahman Sobuz, N.M.S. Hasan, N. Tamanna, M.S. Islam, Structural lightweight  
833 concrete production by using oil palm shell, *Journal of Materials* 2014 (2014).
- 834 [30] M. Mannan, J. Alexander, C. Ganapathy, D. Teo, Quality improvement of oil palm shell  
835 (OPS) as coarse aggregate in lightweight concrete, *Building and Environment* 41(9) (2006)  
836 1239-1242.
- 837 [31] P. Shafigh, M.Z. Jumaat, H. Mahmud, Mix design and mechanical properties of oil palm  
838 shell lightweight aggregate concrete: a review, *International journal of the physical sciences*  
839 5(14) (2010) 2127-2134.
- 840 [32] M. Duque-Acevedo, L.J. Belmonte-Ureña, F.J. Cortés-García, F. Camacho-Ferre,  
841 *Agricultural waste: Review of the evolution, approaches and perspectives on alternative uses,*  
842 *Global Ecology and Conservation* 22 (2020) e00902.
- 843 [33] D. Teo, M.A. Mannan, V. Kurian, C. Ganapathy, Lightweight concrete made from oil  
844 palm shell (OPS): structural bond and durability properties, *Building and Environment* 42(7)  
845 (2007) 2614-2621.

846 [34] M. Mannan, C. Ganapathy, Long-term strengths of concrete with oil palm shell as coarse  
847 aggregate, *Cement and Concrete Research* 31(9) (2001) 1319-1321.

848 [35] A.M. Neville, *Properties of concrete*, 1995.

849 [36] P. Shafigh, M.Z. Jumaat, H.B. Mahmud, N.A.A. Hamid, Lightweight concrete made from  
850 crushed oil palm shell: Tensile strength and effect of initial curing on compressive strength,  
851 *Construction and Building Materials* 27(1) (2012) 252-258.

852 [37] K.H. Mo, T.S. Chin, U.J. Alengaram, M.Z. Jumaat, Material and structural properties of  
853 waste-oil palm shell concrete incorporating ground granulated blast-furnace slag reinforced  
854 with low-volume steel fibres, *Journal of Cleaner Production* 133 (2016) 414-426.

855 [38] E. Serri, M. Suleiman, M.O. Mydin, The effect of curing environment on oil palm shell  
856 lightweight concrete mechanical properties and thermal conductivity, *Advances in*  
857 *Environmental Biology* 9(4) (2015) 222-225.

858 [39] M.K. Yew, H. Bin Mahmud, B.C. Ang, M.C. Yew, Effects of oil palm shell coarse  
859 aggregate species on high strength lightweight concrete, *The Scientific World Journal* 2014  
860 (2014).

861 [40] M.N.A.A. Zawawi, K. Muthusamy, A.P.A. Majeed, R.M. Musa, A.M.A. Budiea,  
862 Mechanical properties of oil palm waste lightweight aggregate concrete with fly ash as fine  
863 aggregate replacement, *Journal of Building Engineering* 27 (2020) 100924.

864 [41] H. Prayuda, F. Saleh, T.I. Maulana, F. Monika, Fresh and mechanical properties of self-  
865 compacting concrete with coarse aggregate replacement using Waste of Oil Palm Shell, *The*  
866 *7th AIC-ICMR on Science and Engineering* 352 (2018).

867 [42] W.W.S. Chai, D.T.C. Lee, C.K. Ng, Improving the properties of oil palm shell (OPS)  
868 concrete using polyvinyl alcohol (PVA) coated aggregates, *Advanced Materials Research*,  
869 *Trans Tech Publ*, 2014, pp. 147-152.

870 [43] Y.B. Traore, A. Messan, K. Hannawi, J. Gerard, W. Prince, F. Tsobnang, Effect of oil  
871 palm shell treatment on the physical and mechanical properties of lightweight concrete,  
872 *Construction and Building Materials* 161 (2018) 452-460.

873 [44] M. Mannan, H. Basri, M.F.M. Zain, M. Islam, Effect of curing conditions on the properties  
874 of OPS-concrete, *Building and Environment* 37(11) (2002) 1167-1171.

875 [45] J. Zhang, D. Li, Y. Wang, Predicting uniaxial compressive strength of oil palm shell  
876 concrete using a hybrid artificial intelligence model, *Journal of Building Engineering* 30 (2020)  
877 101282.

878 [46] E. Fanijo, A.J. Babafemi, O. Arowojolu, Performance of laterized concrete made with  
879 palm kernel shell as replacement for coarse aggregate, *Construction and Building Materials*  
880 250 (2020) 118829.

881 [47] P. Shafigh, M.Z. Jumaat, H. Mahmud, Oil palm shell as a lightweight aggregate for  
882 production high strength lightweight concrete, *Construction and Building Materials* 25(4)  
883 (2011) 1848-1853.

884 [48] J.N. Farahani, P. Shafigh, B. Alsubari, S. Shahnazar, H.B. Mahmud, Engineering  
885 properties of lightweight aggregate concrete containing binary and ternary blended cement,  
886 *Journal of Cleaner Production* 149 (2017) 976-988.

887 [49] U.J. Alengaram, H. Mahmud, M.Z. Jumaat, Enhancement and prediction of modulus of  
888 elasticity of palm kernel shell concrete, *Materials & Design* 32(4) (2011) 2143-2148.

889 [50] P. Shafigh, M.A. Nomeli, U.J. Alengaram, H.B. Mahmud, M.Z. Jumaat, Engineering  
890 properties of lightweight aggregate concrete containing limestone powder and high volume fly  
891 ash, *Journal of Cleaner Production* 135 (2016) 148-157.

892 [51] U.J. Alengaram, H. Mahmud, M.Z. Jumaat, Comparison of mechanical and bond  
893 properties of oil palm kernel shell concrete with normal weight concrete, *International Journal*  
894 *of Physical Sciences* 5(8) (2010) 1231-1239.

895 [52] P. Shafigh, U. Johnson Alengaram, H.B. Mahmud, M.Z. Jumaat, Engineering properties  
896 of oil palm shell lightweight concrete containing fly ash, *Materials & Design* 49(Supplement  
897 C) (2013) 613-621.

898 [53] B. Vakhshouri, S. Nejadi, Mix design of light-weight self-compacting concrete, *Case  
899 Studies in Construction Materials* 4 (2016) 1-14.

900 [54] J.A. Bogas, A. Gomes, M.F.C. Pereira, Self-compacting lightweight concrete produced  
901 with expanded clay aggregate, *Construction and Building Materials* 35 (2012) 1013-1022.

902 [55] M. Hubertová, R. Hela, Durability of Lightweight Expanded Clay Aggregate Concrete,  
903 *Procedia Engineering* 65 (2013) 2-6.

904 [56] T. Uygunoğlu, İ.B. Topçu, Thermal expansion of self-consolidating normal and  
905 lightweight aggregate concrete at elevated temperature, *Construction and Building Materials*  
906 23(9) (2009) 3063-3069.

907 [57] C.G. Papanicolaou, M.I. Kaffetzakis, Pumice aggregate self-compacting concrete  
908 (PASCC), *Proceedings of SCC2010, Montreal* (2010) 1286-1295.

909 [58] Ö. Andiç-Çakır, S. Hızal, Influence of elevated temperatures on the mechanical properties  
910 and microstructure of self consolidating lightweight aggregate concrete, *Construction and  
911 Building Materials* 34 (2012) 575-583.

912 [59] M.I. Kaffetzakis, C.G. Papanicolaou, Mix Proportioning method for lightweight aggregate  
913 SCC (LWASCC) based on the optimum packing point concept, *Innovative Materials and  
914 Techniques in Concrete Construction, Springer*2012, pp. 131-151.

915 [60] M.C. Nepomuceno, L. Pereira-de-Oliveira, S.F. Pereira, Mix design of structural  
916 lightweight self-compacting concrete incorporating coarse lightweight expanded clay  
917 aggregates, *Construction and Building Materials* 166 (2018) 373-385.

918 [61] N.N. Hilal, M.F. Sahab, T.K.M. Ali, Fresh and Hardened Properties of Lightweight Self-  
919 Compacting Concrete Containing Walnut Shells as Coarse Aggregate, *Journal of King Saud  
920 University-Engineering Sciences* (2020).

921 [62] C. Shi, Y. Wu, Mixture proportioning and properties of self-consolidating lightweight  
922 concrete containing glass powder, *ACI Materials Journal* 102(5) (2005) 355-363.

923 [63] T. Lo, P. Tang, H. Cui, A. Nadeem, Comparison of workability and mechanical properties  
924 of self-compacting lightweight concrete and normal self-compacting concrete, *Materials  
925 Research Innovations* 11(1) (2007) 45-50.

926 [64] J. Kanadasan, H.A. Razak, Mix design for self-compacting palm oil clinker concrete based  
927 on particle packing, *Materials & Design* 56 (2014) 9-19.

928 [65] J. Kanadasan, H. Abdul Razak, Engineering and sustainability performance of self-  
929 compacting palm oil mill incinerated waste concrete, *Journal of Cleaner Production* 89 (2015)  
930 78-86.

931 [66] N. Bouzoubaa, M. Lachemi, Self-compacting concrete incorporating high volumes of  
932 class F fly ash: Preliminary results, *Cement and Concrete Research* 31(3) (2001) 413-420.

933 [67] J. Khatib, Performance of self-compacting concrete containing fly ash, *Construction and  
934 Building Materials* 22(9) (2008) 1963-1971.

935 [68] P. Ramanathan, I. Baskar, P. Muthupriya, R. Venkatasubramani, Performance of self-  
936 compacting concrete containing different mineral admixtures, *KSCE Journal of Civil  
937 Engineering* 17(2) (2013) 465-472.

938 [69] M. Jalal, A. Pouladkhan, O.F. Harandi, D. Jafari, Comparative study on effects of Class F  
939 fly ash, nano silica and silica fume on properties of high performance self compacting concrete,  
940 *Construction and Building Materials* 94 (2015) 90-104.

941 [70] M. Liu, Self-compacting concrete with different levels of pulverized fuel ash, *Construction  
942 and Building Materials* 24(7) (2010) 1245-1252.

943 [71] C.D. Atiş, High-volume fly ash concrete with high strength and low drying shrinkage,  
944 *Journal of materials in civil engineering* 15(2) (2003) 153-156.

945 [72] T. Ting, M. Rahman, H. Lau, Compressive Strength of OPS based Self-compacting  
946 Concrete Incorporated with Fly Ash under Elevated Temperature, IOP Conference Series:  
947 Materials Science and Engineering, IOP Publishing, 2019, p. 012086.

948 [73] ASTM, ASTM C150/C150M-12: Standard specification for Portland cement, ASTM  
949 International West Conshohocken, PA, USA, 2012.

950 [74] ASTM, ASTM C127-15: Standard Test Method for Relative Density (Specific Gravity)  
951 and Absorption of Coarse Aggregate, ASTM International, West Conshohocken, PA, 2015,  
952 [www.astm.org](http://www.astm.org), 2015.

953 [75] A. C330/330M, ASTM C330/330M, Standard specification for Lightweight Aggregates  
954 for structural concrete, ASTM International, West Conshohocken, 2017.

955 [76] ASTM, ASTM C128-15: Standard Test Method for Relative Density (Specific Gravity)  
956 and Absorption of Fine Aggregate, ASTM International, West Conshohocken, PA, 2015,  
957 [www.astm.org](http://www.astm.org), 2015.

958 [77] ASTM, ASTM C494 / C494M-17, Standard Specification for Chemical Admixtures for  
959 Concrete, ASTM International, West Conshohocken, PA, 2017, [www.astm.org](http://www.astm.org), 2017.

960 [78] P.S.-C.C.F. Team, Interim guidelines for the use of self-consolidating concrete in PCI  
961 member plants, PCI Journal 48(3) (2003) 14-18.

962 [79] ASTM, ASTM C39 / C39M-18, Standard Test Method for Compressive Strength of  
963 Cylindrical Concrete Specimens, ASTM International, West Conshohocken, PA, 2018,  
964 [www.astm.org](http://www.astm.org), 2018.

965 [80] B.S. Institutions, Method for Determination of Compressive Strength of Concrete Cubes  
966 (BS 1881-116: 1983), London, 2003.

967 [81] A. Norma, C496/C496M-11, Standard test method for splitting tensile strength of  
968 cylindrical concrete specimens, ASTM International, West Conshohocken, PA (2004) 469-90.

969 [82] ASTM, ASTM C567 / C567M-14, Standard Test Method for Determining Density of  
970 Structural Lightweight Concrete, ASTM International, West Conshohocken, PA, 2014,  
971 [www.astm.org](http://www.astm.org), 2014.

972 [83] ASTM, ASTM C642-13, Standard Test Method for Density, Absorption, and Voids in  
973 Hardened Concrete, ASTM International, West Conshohocken, PA, 2013, [www.astm.org](http://www.astm.org),  
974 2013.

975 [84] M. Glavind, E. Pedersen, Packing calculations applied for concrete mix design, Utilizing  
976 Ready Mixed Concrete and Mortar: Proceedings of the International Conference Held at the  
977 University of Dundee, Scotland, UK on, 1999, p. 121.

978 [85] C. BIBM, E. ERMCO, EFNARC. 2005. The European guidelines for Self-compacting  
979 concrete: specification, production and use, SCC European Project Group (2005).

980 [86] ASTM, ASTM C29 / C29M-17a, Standard Test Method for Bulk Density (“Unit Weight”)  
981 and Voids in Aggregate, ASTM International, West Conshohocken, PA, 2017, [www.astm.org](http://www.astm.org),  
982 2017.

983 [87] R.W. Floyd, W.M. Hale, J.C. Bymaster, Effect of aggregate and cementitious material on  
984 properties of lightweight self-consolidating concrete for prestressed members, *Construction*  
985 *and Building Materials* 85 (2015) 91-99.

986 [88] J. Li, Y. Chen, C. Wan, A mix-design method for lightweight aggregate self-compacting  
987 concrete based on packing and mortar film thickness theories, *Construction and Building*  
988 *Materials* 157 (2017) 621-634.

989 [89] A. Yahia, M. Tanimura, A. Shimabukuro, Y. Shimoyama, T. Tochigi, Effect of mineral  
990 admixtures on rheological properties of equivalent self-compacting concrete mortar, *Proc.*, 7th  
991 East Asia-Pacific Conf. on Structural Engineering and Construction, COMS Engineering Corp.  
992 Japan, 1999, pp. 559-564.

- 993 [90] ASTM, ASTM C330 / C330M-17a, Standard Specification for Lightweight Aggregates  
994 for Structural Concrete, ASTM International, West Conshohocken, PA, 2017, [www.astm.org](http://www.astm.org),  
995 2017.
- 996 [91] R.H. Kupaei, U.J. Alengaram, M.Z.B. Jumaat, H. Nikraz, Mix design for fly ash based oil  
997 palm shell geopolymer lightweight concrete, *Construction and Building Materials* 43 (2013)  
998 490-496.
- 999 [92] A. Lotfy, K.M.A. Hossain, M. Lachemi, Mix design and properties of lightweight self-  
1000 consolidating concretes developed with furnace slag, expanded clay and expanded shale  
1001 aggregates, *Journal of Sustainable Cement-Based Materials* 5(5) (2015) 297-323.
- 1002 [93] Mahmud, M. Jumaat, U. Alengaram, Influence of sand/cement ratio on mechanical  
1003 properties of palm kernel shell concrete, *Journal of Applied Sciences* 9(9) (2009) 1764-1769.
- 1004 [94] B. Felekoğlu, S. Türkel, B. Baradan, Effect of water/cement ratio on the fresh and  
1005 hardened properties of self-compacting concrete, *Building and Environment* 42(4) (2007)  
1006 1795-1802.
- 1007 [95] A.K. Saha, Effect of class F fly ash on the durability properties of concrete, *Sustainable*  
1008 *environment research* 28(1) (2018) 25-31.
- 1009 [96] A. Fraay, J. Bijen, Y. De Haan, The reaction of fly ash in concrete a critical examination,  
1010 *Cement and concrete research* 19(2) (1989) 235-246.
- 1011 [97] P. Chindapasirt, C. Chotithanorn, H. Cao, V. Sirivivatnanon, Influence of fly ash fineness  
1012 on the chloride penetration of concrete, *Construction and Building Materials* 21(2) (2007) 356-  
1013 361.
- 1014 [98] R. Kurda, J. de Brito, J.D. Silvestre, Water absorption and electrical resistivity of concrete  
1015 with recycled concrete aggregates and fly ash, *Cement and Concrete Composites* 95 (2019)  
1016 169-182.
- 1017 [99] J.H. Filho, M.d. Medeiros, E. Pereira, P. Helene, G. Isaia, High-volume fly ash concrete  
1018 with and without hydrated lime: chloride diffusion coefficient from accelerated test, *Journal of*  
1019 *materials in civil engineering* 25(3) (2012) 411-418.

1020